STRENGTH AND FAILURE ANALYSIS OF COMPOSITE LAMINATE CONTAINING A CIRCULAR HOLE WITH REINFORCEMENT

THESIS

Jong Hee Lee
Captain, ROKAF

AFIT/GAE/AA/87D-9

DEPARTMENT OF THE AIR FORCE
AIR UNIVERSITY
AIR FORCE INSTITUTE OF TECHNOLOGY

Wright-Patterson Air Force Base, Ohio

STRENGTH AND FAILURE ANALYSIS OF COMPOSITE LAMINATE CONTAINING A CIRCULAR HOLE WITH REINFORCEMENT

THESIS

Jong Hee Lee
Captain, ROKAF

AFIT/GAE/AA/87D-9

Approved for public release; distribution unlimited

AFIT/GAE/AA/87D-9

STRENGTH AND FAILURE ANALYSIS OF COMPOSITE LAMINATE CONTAINING A CIRCULAR HOLE WITH REINFORCEMENT

THESIS

Presented to the Faculty of the School of Engineering
of the Air Force Institute of Technology
Air University
In Partial Fulfillment of the
Requirements for the Degree of
Master of Science in Aeronautical Engineering

Jong Hee Lee, B.S.
Captain, Republic of Korea Air Force

December 1987

Preface

In the present study, the notched strength of a composite laminate containing a circular hole with reinforcement was analyzed experimentally through tension and compression test. Three different reinforcing material systems were used by means of adhesive bond and unbonded snug-fit inclusion. To find the effect of reinforcing hole size, four different sizes of hole diameters (0.1", 0.2", 0.4", 0.6") were employed for each material system. To help the complete understanding of the failure mechanism, the whole chronology of failure progression was also investigated using microscope and X-ray inspection. It is hoped that the results presented in this thesis will increase the understanding of fracture in composite structures containing reinforced hole. As with any large project which is individually undertaken, this study involved the assistance of many other individuals,some of whom I must single out. I am indebted to Dr. Stephan W. Tsai who sponsored this project, Dr. S. C. Tan for his help in theoretical analysis and discussions, and Dr. R. Y. Kim of the University of Dayton Research Institute. I also thank the AFIT laboratory technical staff and especially Mr. Jay Anderson for his help. I am especially indebted to Dr. Shankar Mall who was always available with his able assistance and guidance throughout this long endeavor. My most special thanks to my wife, Seunghee and my son Wangsok, who endured me during this project.

Jong Hee Lee

Table of Contents

List of Figures

List of Tables

List of Symbols

a_{ij}	In-plane compliance components of the laminated plate
a'_{ij}	Compliances of the inclusion
a_1	Characteristic length of Effective Average Stress Model
b_0	Characteristic distance of Minimum Strength Model
b_1	Characteristic distance of Effective Point Stress Model
F^*_{12}	Stress interaction term of Tsai-Wu quadratic failure criterion
Q_{ij}	Lamina Stiffness
$\bar{S}_{ij}$	Lamina Compliance
X	Longitudinal tensile strength of a lamina
X'	Longitudinal compression strength of a lamina
λ	Opening aspect ratio
$\{\sigma\}$	Overall stresses of a given ply
$\{\sigma^\circ\}$	Stresses due to uniform stress field
$\{\sigma^*\}$	Stresses due to opening
σ'_i	Stresses for the inclusion in the laminate axes
σ_a	Normal stress at the point $(0, a_1)$
σ_n	Ultimate stress of notched laminate
σ_0	Ultimate stress of unnotched laminate
σ_p	Normal stress at the point $(0, b_1)$ across y-plane
$\bar{\sigma}_x$	Applied stress in Effective Point Stress model

Abstract

Tension and compression tests of quasi-isotropic, $[0/\pm 45/90]_{2s}$, graphite/epoxy laminate containing circular hole with reinforcement was conducted using Instron static testing machine. Two types of reinforcement boundary conditions were investigated; adhesive bonded reinforcement and snug-fit unbonded plug. For each case of bondary conditions, four different sizes of hole diameter (0.1", 0.2", 0.4", 0.6") and three types of reinforcing material (aluminum, plexiglass, steel) were employed for investigation.

The experiments were mainly focused on the evaluation of ultimate strength of reinforced panel relative to the case of open hole. In addition to this, failure mechanism analysis for both boundary conditions were studied. To help designers and users of composite, previously available theoretical fracture models and their comparison with the present experimental results are also discussed.

STRENGTH AND FAILURE ANALYSIS OF COMPOSITE LAMINATE CONTAINING A CIRCULAR HOLE WITH REINFORCEMENT

I. Introduction

The use of advanced composite materials has grown in recent years to the extent that it is included in nearly every program of aerospace structures. The maintenance and repair of these structures is now becoming the concern of the users as well as the manufacturers of the aerospace vehicle. Various repair concepts of composites are available which include a wide range of approaches from highly refined and structurally efficient but expensive flush patch repairs to external mechanically attached metal patch repairs. In all these repair methods, one of the several concerns is the prediction of the strength of repaired laminates. The present study is focused in this direction.

Out of various kinds of repairing method, the one selected for this study is an idealized case which simulates a practical situation where a damaged laminate has been repaired by drilling a hole and thereafter plugging the hole with a reinforcement. Therefore, the present study involves the investigation of a composite laminate containing a circular hole with a reinforcement. This is a first step

towards the investigation of more sophisticated repair methods.

The presence of hole in plate, which is subjected to in-plane loads, produces stress concentrations around that hole and consequently weakening of the plate. Moreover, the tensile strength reduction has been observed to depend on the hold size, i.e. larger holes cause greater strength reduction than smaller holes and this phenomenon that has become known as the "hole-size-effect" cannot be accounted by a classical stress concentration factor. The various method of reducing the stress concentrations by local reinforcements have been extensively investigated for circular, elliptical, and rectangular holes in isotropic plates (1). However with increasing use of anisotropic material these problems have become more acute. Where as for a hole in an infinite isotropic plate subjected to uniaxial tension the maximum stress concentration factor is 3 (2), in the case of fiber reinforced composite plate, for example, with all the fibers in the direction of the load the stress concentration factor is about 9 (3), depending on the degree of orthotropy present.

The problem of predicting notched strength of a composite laminate containing a circular or elliptical hole has been considered by several investigators (4-8). However, very few studies have been reported for the evaluation of strength for composite laminate containing

circular hole with reinforcement. Kocher and Cross (9) investigated the reinforced cutouts in composite laminates. These reinforcements were cocured with the composite laminate so as to form an integral part of the structure. O'Neill (10), Pickett and Sullivan (11) studied the reinforcement of hole in a very large composite plate (26" long and 10" wide). They employed the reinforcing technique where additional layers of same composite materials of circular shape were cocured on the sides of laminate with hole. Recently, Tan and Tsai (12) have developed a closed form analysis which provides the stress distribution near of reinforced hole in the composite laminate. This analysis has shown that the strength of notched laminate can be drastically increased with the proper selection of reinforcement. However, no experimental verification of this analysis (12) has been reported so far.

The objective of present study was, therefore, to investigate the strength and failure mechanism of composite laminate with a reinforced hole. Two types of reinforcements were studied; (1) a bonded plug reinforcement and (2) snug-fit plug reinforcement. Three materials - steel, aluminum, and plexiglass - were used to plug reinforcements. To investigate the hole size effect, four hole diameters - 0.1", 0.2", 0.4", and 0.6" - were selected. Two types of loading, i.e. tension and compression, were included in this study. The composite material for this

study was graphite/epoxy (AS4/3501-6) with quasi-isotropic $[0/\pm 45/90]_{2s}$ lay-up.

The details and results of these investigations are presented in the successive chapters.

II. Literature Review

There are many difficulties in determining strength reductions for notched composite laminates. The infinite number of possible ply lay-ups, a large variety of fiber and matrix combinations, uncertain failure criteria, the specific applications of geometry (i.e. thickness of the laminate, notch size, thickness-to-hole size ratio, and width-to-hole size ratio, and environmental conditions around the composite) must be considered. Currently, there are several techniques available for prediction of strength reduction in composite laminates containing various types of cut-outs that include cracks, slits, and holes: (1) a finite element method, (2) a fracture mechanics approach, (3) modified isotropic plate theory, and (4) anisotropic plate theory. The discussion here is intended to focus on some of the most popular and useful predictive approaches that have been successfully investigated for notched composite laminates. Also, a literature review is presented about the previous work involving a plate with reinforced hole.

Open Cut-outs

Waddoups, Eisenmann and Karminski (13) were probably the first to suggest a fracture mechanics approach for predicting the static strength of a flawed specimen. They

proposed that the hole size effect on the strength of laminated composites can be explained and accounted if one assumes that the regions of intense stress across the hold diamater can be treated like two symmetrical cracks of a characteristic length "a" emanating from each side of the circular hole perpendicular to the load direction. They analyzed this equivalent problem on the basis of Bowie's (14) solution for the stress intensity factor K_I, and found a reasonable agreement with their experimental results for $(0/90)_s$ graphite/epoxy laminates tested over a range of hole sizes. However, the characteristic length "a" was not constant for all hole sizes and no physical interpretation was given to this dimension.

Cruse (4) modeled a circular hole of radius r as a crack of half length r* and attempted to predict tensile strength of notched composites. The dimension r* was determined by comparing the stress distribution for a circular hole in an orthotropic plate of a finite width with that for a crack in the same material. Having determined the effective crack half length r*, the strength of the laminate was determined by using fracture mechanics in conjunction with the fracture toughness for the material, which was determined from an independent test. This model found only a very limited support when compared with the experimental data for various unidirectional and laminated composites.

Whitney and Nuismer (15) proposed two failure criteria for predicting the uniaxial tensile strength of laminated composites containing through-the-thickness material notches (circular holes and straight cracks) without resorting to the concepts of linear elastic fracture mechanics (LEFM). These criteria are based on the normal stress distribution at the point across the diameter of a hole in an infinite isotropic plate subjected to a uniform tensile stress at the infinity. In the proposed point stress criterion, it is assumed over some distance (d_0) away from the tipof notch reaches the value equal to or greater than the strength of the unnotched material. The second related criteria known as the 'average stress criterion' is based on the assumption that tensile failure of the material will occur when the average stress over some distance (a_0) measured from the notched tip is equal to the unnotched laminate strength. The critical dimension d_0 and a_0 are assumed to be the material properties independent of the laminate construction and specimen size. The experimental data for circular hole is quasi-isotropic glass/epoxy and straight cracks in $(0/\pm 45)_s$ graphite/epoxy laminates showed good correlations with the predictions based on these two failure criteria.

Further experiments by Nuismer and Whitney (16) were carried out on glass/epoxy and graphite/epoxy systems using through-the-thickness circular holes and cracks of several sizes to establish the suitability of these criteria. It was observed that although these two models appeared

reasonable to explain the hole-size effect for various composite systems considered by them, the accuracy of these cannot conclusively be established.

Karlark (6) tested a series of eight-ply symmetric quasi-isotropic graphite/epoxy laminates with a hole of various sizes and analyzed the results by using point stress criterion. He proposed a criteria that "d_0" had a square root dependence on hole sizes. A characteristic factor, k_0, defining the relationship between 'd_0' and the hole diameter was introduced. Although Karlak was able to better fit failure results from Whitney and Kim (17) with his criteria than with the point stress method, he could not assign a physical significance to the square root dependency.

Pipes, Gillipse and Wetherhold (18) introduced a three parameter model to enhance failure prediction. The three parameter model was dependent on (1) the strength of the composite laminate with holes, (2) a notch sensitivity factor 'c', and (3) an exponential factor 'm'. This three parameter model is enhancement of Whitney's two parameter model.

Malik (19) studied about the room and high temperature strength of Gr/PEEK and Gr/Epoxy laminates containing circular holes. Tension and compression tests were done using MTS static test machine and the comparison of the experimental data with predicted failure stress were also shown graphically.

Ramey (20) tried to compare the notch strength of quasi-isotropic Gr/Epoxy containing circular hole with that of Gr/PEEK at elevated temperature. Both tension and compression test were done using MTS machine and addition to that Scanning Electron Microscope (SEM) photographs are used to determine specific notch effects of failure modes.

Tan (21) introduced another approach to predict the failure models for unnotched and notched multi-directional composite laminates. He used three models - effective point stress, effective average stress, and minimum strength model - based on the stress distribution around an opening of multi-directional composite laminates. These models utilize a characteristic length and a proposed failure criterion that requires the longitudinal strength parameters and stress distribution of a lamina within a laminate. Comparisons showed that the ultimate strength predictions for unnotched and notched laminates both agree well with experimental data for graphite/epoxy material system.

Reinforced Hole

An early paper by Gurney (22) gave a plane stress solution for reinforcement of a circular hole by a thin uniform annulus of rectangular cross-section. Later Reissner and Murdochow (23) introduced the concept of a neutral hole, that is where the reinforcement is designed to restore the stresses and displacements in the sheet to the values that would have appeared without the hole. The shape of ideal

reinforcement in the form of a bead was found not to be realizable in practice, so a reinforcement of constant cross-section was investigated. Values of strain were obtained in tests with a plate, and these agreed reasonably well with the theoretical predictions.

Mansfield (24) extended the idea of neutral hole by predicting the shape of the hole and the variation in cross-section of the bead reinforcement for any particular load, such as shear or pure tension. The above ideas, along with other work in this field were used to produce design information in Royal Aeronautical Data Sheet 70005 (1) as mentioned previously.

Seika and Ishii (25) investigated the maximum stress in an isotropic plate with an annular reinforced circular hole under uniaxial tension. They found the relationship between the thickness of plugged annular disks and stress concentration factor around the hole.

Ghosh, Datta and Rao (26) studied pin joints problem in a large sheet. Using three mixed boundary conditions (interference, push, and clearance fit) which can happen in actual application, they solved theoretically the behavior of pin joints under biaxial loading.

Heller, Jones, and Williams (27) presented analytical solutions for the stress analysis of fastener holes with bonded inserts. They used finite element method with fracture mechanics as techniques to study this problem. They found that the stress concentration factors at a hole

significantly reduced if the hole contains a bonded rivet or bonded sleeve.

The reinforcement of holes in multi-directional composites was considered first by Waszczuk and Cruse (28). Bolted bearing specimens, reinforced by local thickening, were examined by finite element method. The plates used were all multi-directional composites, and three failure criteria were considered (maximum stress, maximum strain, and distortional energy).

Kocher and Cross (9) tried to predict the strength of reinforced cutouts in graphite composite structures. The reinforcements tried were metallic discs, square-shaped multi-layer composites, and butterfly-shaped composites. All of them are interleaved with the plies of the panel so as to form an integral part of the structure. Finite element method was used with Tsai-Hill failure criteria. It was shown that up to 90% of the apparent laminate strength (no cutout) could be achieved with the integral composite reinforcements, where weight was only 20-40% of a metal reinforcement of the same loading capacity.

O'Neill (10) studied asymmetric reinforcements of a quasi-isotropic graphite epoxy plate containing a circular hole under uniaxial tension load. He used 26" long and 10" wide $[0/\pm 45/90]_s$ laminate containing 1" diameter hole at center of the panel. It was analyzed by FEM, and experimentally tested. Six different types of asymmetric reinforcements which varied the volume from 94% to 162% of

the volume of material removed by the hole was used. Results of these computation and experiments showed only 5 to 12% recovery of the basic laminate strength. Pickett and Sullivan (11) tried to predict same kind of strength but with symmetric reinforcements. They also used FEM with experiments and through this study they improved ultimate strength from 29 to 40% of unreinforced panel under the same loading condition.

Pradhan and Ray (29) investigated the stress distribution around pin-loaded holes of isotropic as well as several fiber reinforced plastic (FRP) composite materials. They considered the case of full contact (contact angle = 180°) and that of the partial contact (contact angle < 180°) between the pin and the hole. Again they selected FEM for stress analysis and some important results regarding the peak stress distribution around the pin-loaded hole are made especially with respect to the anisotropy (axial to transverse elastic stiffness ratio, E_1/E_2) of material by way of fiber reinforcements and laminating schemes, geometrical parameters (hole diameter to plate with ratio), and contact angle between the pin and hole.

Pradhan and Santra (30) attempted to investigate similar case using FEM, and also annular type disk reinforcements surrounding circular hole of uniaxially loaded FRP composite plates. They established the peak stress value which was affected by the thickness and diameter of reinforcing disks. With increasing thickness of

reinforcing disks, the peak stress values were reduced and, with increase of reinforcing disc diameter, the peak stress values were reduced.

Chang (31) studied about the effect of pin load distribution of pin-loaded holes in laminated composites. Based on his experimental work along with others (32,33), he applied Yamada-Soon failure criteria along with the Chang-Scott-Springer characteristic curve. Using FEM technique, strength and failure modes were calculated for both a cosine load distribution and a load distribution determined by an iterative procedure.

Hyer, Klang and Cooper (34) studied about the effect of pin elasticity, clearance, and friction on the stresses in a pin-loaded orthotropic plate. Two pin stiffnesses, two clearance levels, two friction levels and two laminates, $[0/\pm45/90]_s$ and $[0_2/\pm45]_s$ are studied. The effects of pin elasticity, clearance, and friction on the load capacity of the plate are assessed by comparing the load capacity of the plate with the capacity when pin is rigid, perfectly fitting and frictionless. This study showed that clearance and friction have a significant influence on the distribution of the maximum value of the stresses around the hole.

Tan and Tsai (12) have developed the closed form analysis which provides the stress distribution equations of composite laminate with inclusion. They derived these equations by modifying the stress potential of a laminate with an open hole. Using these equations they plotted the

tangential stress distribution at the material/inclusion boundary for CFRP T300/5208 $[0/\pm 45/90]_s$ laminate. The maximum positive tangential stress occurs on the axis normal to the applied load and the stress concentrations are significantly reduced by inclusions. They also proposed two criteria - First Ply Failure (FPF) and Fiber Failure (FF) - for notched and notched with inclusion. Their comparison with their experimental data for open hole showed excellent agreement. However, they have no comparison with experimental results of reinforced hole. As mentioned previously, author is not aware of any such experimental work, hence the present study was undertaken.

III. Theoretical Background

Awerbuch and Madhukar (35) have collected all available fracture models, reviewed briefly, and presented samples of experimental data for notched composite laminates. Besides those criteria, some of recently developed fracture models were chosen here to assess their suitability for the strength prediction of the present study. These models and their corresponding theory will be discussed in the following section.

Stress Analysis

Tan and Tsai (12) have developed the stress analysis of anisotropic plate containing elliptical opening under biaxial loading conditions. They solved for the stresses based on the complex potential approach presented in Lekhnitskii's Anisotropic Plates (3). The coordinate systems are depicted in Fig. 1 and governing equations are as follow.

For open cutout. Overall stresses of a given infinite anisotropic laminate are as follow:

$$\{\sigma\} = \{\sigma^{\circ}\} + \{\sigma^{*}\}$$

here $\{\sigma^{\circ}\}$ = Stress due to uniform stress field

$\{\sigma^{*}\}$ = Stress due to the opening

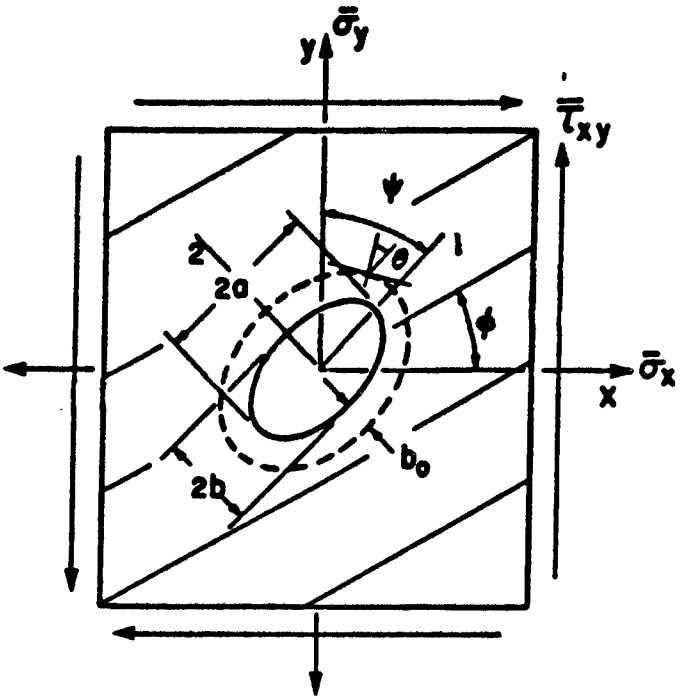

Fig. 1. Coordinates of an Infinite Anisotropic Laminate with an Elliptical Opening.

All the stress components refer to the major and minor axes of ellipse. The relationship between the applied stress field at infinity in the laminate axes 1-2 and that in the axes of the ellipse is given by the following transformation equation

$$\sigma_1^\circ = \sigma_1 \sin^2\psi + \sigma_2 \cos^2\psi + \sigma_6 \sin 2\psi$$

$$\sigma_2^\circ = \sigma_1 \cos^2\psi + \sigma_2 \sin^2\psi - \sigma_6 \sin 2\psi \qquad (2)$$

$$\sigma_6 0 = -(\sigma_1 - \sigma_2) \sin\psi \cos\psi - \sigma_6 \cos 2\psi$$

Using complex potential technique (3) the stress field due to the opening is

$$\sigma_1^* = \mathrm{Re}[(\mu_1^2 f_1 g_2 - \mu_2^2 f_2 g_1)/(\mu_1 - \mu_2)]$$

$$\sigma_2^* = \mathrm{Re}[(f_1 g_2 - f_2 g_1)/(\mu_1 - \mu_2)] \qquad (3)$$

$$\sigma_6^* = \mathrm{Re}[-(\mu_1 f_1 g_2 - \mu_2 f_2 g_1)/(\mu_1 - \mu_2)]$$

where

$$f_j = (1-i\mu_j\lambda)/[\beta\sqrt{\beta^2-1-\mu_j^2\lambda^2} + \beta^2-1-\mu_j^2\lambda^2] \qquad (4)$$

$$g_j = -(1-i\mu_j\lambda)\sigma_6^0 - \mu_j\sigma_2^0 + i\lambda\sigma_1^0 \qquad (5)$$

$$j = 1,2$$

$$\beta = (1+\alpha)\cos\theta + \mu_j(\lambda + \alpha)\sin\theta \qquad (6)$$

$$\lambda = b/a \qquad \alpha = b_0/a \qquad (7)$$

where b_0 is the characteristic dimension measured radially outward from the opening contour to the characteristic curve and it can be determined by semi-empirically.

The complex roots μ_j represent the solution of the following characteristic equation:

$$a_{11}\mu^4 - 2a_{16}\mu^3 + (2a_{12} + a_{66})\mu^2 - 2a_{26}\mu + a_{22} = 0 \qquad (8)$$

where a_{ij} is the in-plane compliance components of the laminated plate. For an orthotropic plate, $a_{16} = a_{26} = 0$, and equation (8) becomes

$$a_{11}\mu^4 + (2a_{12} + a_{66})\mu^2 + a_{22} = 0 \qquad (9)$$

For a square symmetric plate, $a_{11} = a_{22}$, and equation (8) becomes

$$a_{11}\mu^4 + (2a_{12} + a_{66})\mu^2 + a_{11} = 0 \qquad (10)$$

For an isotropic plate, equation (8) becomes

$$\mu^4 + 2\mu^2 + 1 = 0 \qquad (11)$$

Laminate with Inclusion. The stress distribution of an anisotropic laminate with a rigid inclusion can be expressed in a form similar to the open hole solution. The solution is given for the case when the principal axis of the elliptical inclusion coincide with the laminate axis, i.e. $\psi = 90°$. The relationship described by equations (1) through (4) remain valid for determining the stress distribution for the base laminate. The function g_j of equation (5) is modified to:

$$g_j = (\sigma_1^0 - \sigma_1')\lambda_i - (\sigma_2^0 - \sigma_2')\mu_j - (\sigma_6^0 - \sigma_6')(1-{}_i\mu_j\lambda) \qquad (12)$$

where $j = 1,2$ and σ_1', σ_2', σ_6' are the stresses for the inclusion in the laminate axes.

The stress for the inclusion can be written explicitly as

$$\sigma'_1 = (\sigma_1^0/D_1)[a_{11}a_{22}(k+n)+a_{11}a'_{22}k(1+n)+a_{22}(a_{12}+a_{66}+a'_{12})]$$

$$+(\sigma_2^0/D_2)[a_{11}(a_{22}-a'_{22})+a_{22}(a_{12}-a'_{12})(n+k)/k^2]$$

$$\sigma'_2 = (\sigma_1^0/D_1)[a_{22}(a_{11}-a'_{11})+a_{11}(a_{12}-a'_{12})k(1+n)]+(\sigma_2^0/D_2)$$

$$[a_{11}a_{22}(1+n)/k+a_{22}a'_{11}(n+k)/k^2+a_{11}(a_{12}+a_{66}+a'_{12})]$$

$$\sigma'_6 = (\sigma_6^0/D_6)[a_{11}nk+(2a_{12}+a_{66})k+a_{22}(2+n)] \qquad (13)$$

where

a_{ij} = compliances of the base laminate

a'_{ij} = compliances of the inclusion

$i,j = 1,2,6$

and

$$D_1 = (a_{11}a_{22}+a'_{11}a'_{22})k+a_{22}(a_{66}+2a'_{12})+(a_{11}a'_{22}k+a_{22}a'_{11})n$$

$$-(a_{12}-a'_{12})^2k$$

$$D_2 = (a_{11}a_{22}+a'_{11}a'_{22})/k+a_{11}(a_{66}+2a'_{12})+(a_{22}a'_{11}/k+a_{11}a'_{22})$$

$$n/k-(a_{12}-a'_{12})^2/k$$

$$D_6 = a_{11}kn+(2a_{12}+a'_{66})k+a_{22}/(2+n) \qquad (14)$$

where

$$k = -\mu_1\mu_2 = \sqrt{a_{22}/a_{11}} \tag{15}$$

$$n = -i(\mu_1+\mu_2) = \sqrt{(2a_{12}+a_{66})/a_{11}} + 2\sqrt{a_{22}/a_{11}} \tag{16}$$

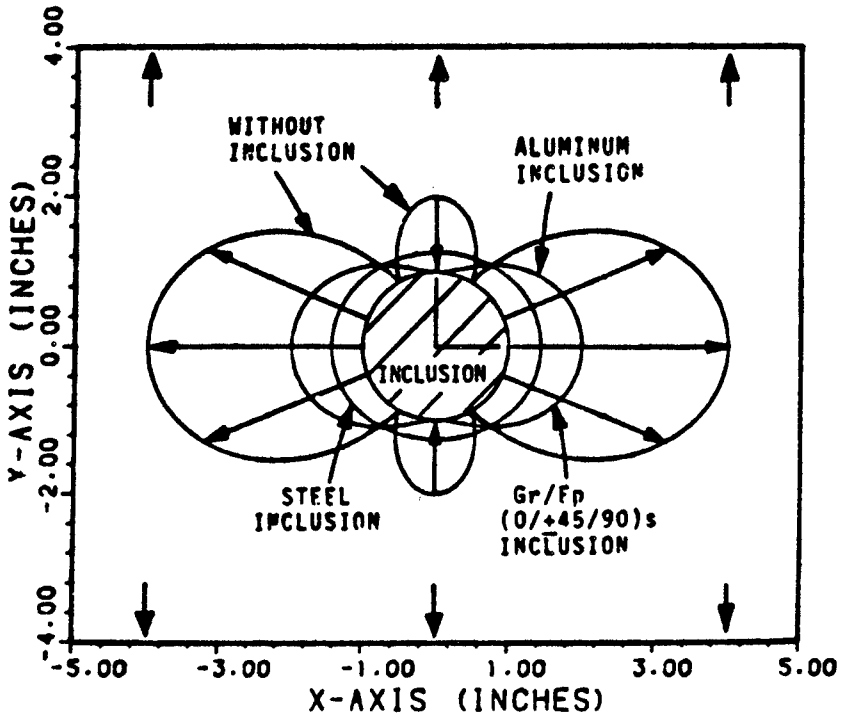

Fig. 2. The Tangential Stress Concentration at the Interphase Boundary of the GR/EP $[0/\pm45/90]_s$ Laminate Containing a Circular Inclusion from Ref. 12.

An example that utilizes the above equations is illustrated in Fig. 2. The tangential stress at the base material/inclusion boundary is plotted for the CFRP T300/5208 $[0/\pm45/90]_s$ laminate at room temperature. The maximum positive tangential stress occurs on the axis normal to the applied load. The stress concentrations, shown for

four cases in Fig. 2, are equal to (1) 3 in the absence of any inclusion, (2) 1.004 for aluminum inclusion, (3) 1 for a CFRP $\pi/4$ laminate inclusion, and (4) 1.44 for steel inclusion.

Fracture Criteria

Before considering notched strength prediction models, two criteria which can be applied to these strength prediction models are described in the following. To find the ratio of notched and unnotched laminate strength, a Strength Reduction Factor (SRF) is defined as:

SRF = Notched Strength/Unnotched Strength

First Ply Failure Criterion (FPF). The Tsai-Wu quadratic failure criterion with the stress interaction term $F^*_{12} = -0.5$ is applied to the First Ply Failure (FPF) analysis. The SRF is computed by the First Ply strength at a characteristic distance for a notched laminate divided by the First Ply strength of an unnotched laminate, i.e.

$$SRF = \frac{\text{FPF (Notched laminate at given characteristic length)}}{\text{FPF (Unnotched laminate)}}$$

Fiber Failure Criterion (FF). Tan (37) has proposed that when the fiber strength at a given characteristic distance from the discontinuity of a laminate is equal to or greater than the fiber strength of the corresponding

unnotched laminate, the laminate is assumed to have failed. This criterion is based on a quadratic form of failure which utilizes the tensile and compressive strength properties and stress distribution across the fiber:

$$\frac{\sigma_1^2}{XX'} + \sigma_1\left(\frac{1}{X} - \frac{1}{X'}\right) = e_f \qquad (17)$$

where σ_1 is lamina normal stress along the fiber direction and X, X' are longitudinal tensile and compressive strength of lamina, respectively. If any ply satisfies the condition; $e_f \geq 1$, the laminate would fail, i.e. it can no longer carry any load. Hence, in this case, Strength Reduction Factor is:

$$SRF = \frac{FF \text{ (Notched laminate at a given characteristic length)}}{FF \text{ (Unnotched laminate)}}$$

Notched Strength Prediction Models

Two criteria, explained above, were used in the following three models to predict the strength of laminate with a reinforced hole.

Effective Point Stress Model (EPS). Approximate stress distribution of an infinite orthotropic symmetric laminate containing an elliptical opening has been derived by Tan (37). The coordinate system is shown in Fig. 3, and the result is given in the following.

$$\frac{\sigma_p}{\bar{\sigma}_x} = 1 + \frac{1}{\sqrt{\xi_1^{-2}-1+\lambda^2}\,(\xi_1^{-1}+\sqrt{\xi_1^{-2}-1+\lambda^2})} + \frac{\lambda^2(1+\lambda)(\xi_1^{-1}+2\sqrt{\xi_1^{-2}-1+\lambda^2})}{(\xi_1^{-2}-1+\lambda^2)^{3/2}(\xi_1^{-1}-1+\lambda^2)^2}$$

$$- \frac{\lambda^7}{2}(K_T^{\infty}-1-\frac{2}{\lambda})\left[\frac{5\xi_1^{-1}}{(\xi_1^{-2}-1+\lambda^2)} - \frac{7\lambda^2\xi_1^{-1}}{(\xi_1^{-2}-1+\lambda^2)^{a/2}}\right] \qquad (18)$$

where σ_p, and $\bar{\sigma}_x$, are the normal stress at the point $(0,b_1)$ across y-plane and the applied stress, respectively, and

$$\lambda = b/a \qquad (19a)$$

$$\xi_1 = a/(a+b_1) \qquad (19b)$$

$$K_T^{\infty} = 1 + \frac{1}{\lambda}\sqrt{\frac{2}{A_{22}}\left(\sqrt{A_{11}A_{22}} - A_{12} + \frac{A_{11}A_{22}-A_{12}^2}{}\right)} \qquad (19c)$$

where λ denotes the opening aspect ratio of the major and minor diameters, 2a and 2b respectively. The b_1 is a characteristic length to be determined empirically and A_{ij}, $i,j = 1,2,6$ designate the in-plane stiffness of the laminate with 1 and 2 in the directions parallel and transverse to the applied load, respectively.

For circular openings, $\lambda = 1$, Eq. (18) is reduced to

$$\frac{\sigma_p}{\sigma_x} = \{2+\xi_1^2+3\xi_1^4-K_T^{\infty}-3)(5\xi_1^6-7\xi_1^8)\}\ /2 \qquad (20)$$

and for cracks, $\lambda = 0$, Eq. (18) is reduced to

$$\frac{\sigma_p}{\sigma_x} = 1/\sqrt{1-\xi_1^2} \tag{21}$$

Once the laminate stress is obtained, the ply stress can be obtained using the classical laminated plate theory.

$$\sigma_1/\sigma_p = (Q_{11}\bar{S}_{11}+Q_{12}\bar{S}_{12})\cos^2\phi+(Q_{12}\bar{S}_{11}+Q_{22}\bar{S}_{12})\sin^2\phi$$

$$+ 2(Q_{16}\bar{S}_{11}+Q_{26}\bar{S}_{12})\sin\phi\cos\phi \tag{22}$$

where Q_{ij} : laminate stiffness

$\bar{S}_{ij}$: laminate compliance

$i,j = 1,2,6$

σ_1 = lamina normal stress in the fiber direction.

The SRF is calculated from

$$\text{SRF} = \frac{\text{FPF or FF (Notched) at } (0,b_1)}{\text{FPF or FF (Unnotched)}}$$

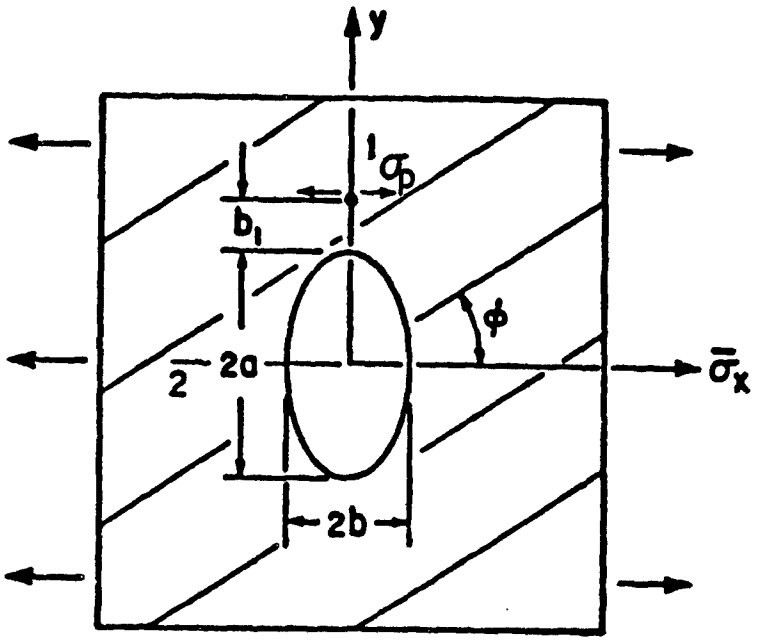

Fig. 3. Characteristic Length, b_1, of the Effective Point Stress Model.

Effective Average Stress Model (EAS). The averaged laminate stress, σ_a, over a distance, a_1, away from the elliptical opening and on the axis normal to the applied load has shown in Fig. 4 and derived as follow (36).

$$\frac{\sigma_a}{\sigma_x} = \frac{\lambda^2}{(1-\lambda)^2}\,\xi_2^{-1} + \frac{(1-2\lambda)}{(1-\lambda)^2}\sqrt{\xi_2^{-2}-1+\lambda^2} - \frac{\lambda^2}{(1-\lambda)\sqrt{\xi_2^{-2}-1+\lambda^2}} \quad (23)$$

$$+ \frac{\lambda^2}{2}\,(K_T^{\infty}-1-\frac{2}{\lambda})\left[(\xi_2^{-2}-1+\lambda^2) - \lambda^2(\xi_2^{-2}-1+\lambda^2)^{-7/2}\right]$$

where λ and K_T^{∞} have been defined in Eq. (19a) and (19c), respectively, and

$$\xi_2 = \frac{a}{a+a_1} \tag{24}$$

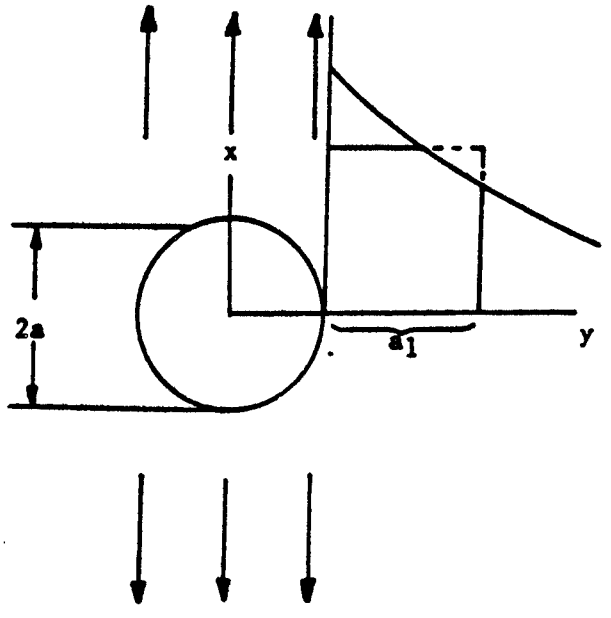

Fig. 4. Characteristic Length, a_1, of the Effective Average Stress Model.

The value of a_1 will be determined empirically. For circular opening, $\lambda = 1$, Eq. (23) is reduced to

$$\frac{\sigma_a}{\sigma_x} = \{2-\xi_2^2-\xi_2^4+(K_T^{\infty}-3)(\xi_2^6-\xi_2^8)\}/2(1-\xi_2) \tag{25}$$

For a center normal crack, Eq. (23) is reduced to

$$\frac{\sigma_a}{\bar{\sigma}_x} = \sqrt{\frac{\xi_2^{-1} + 1}{\xi_2^{-1} - 1}} \tag{26}$$

Note that if the average stress fracture model is applied on a laminate basis, σ_a and $\bar{\sigma}_x$ of Eq. (23) are replaced by σ_n^∞ and σ_n^∞, respectively.

The average stress of each ply over a characteristic distance in the fiber direction can be obtained using the classical laminated plate theory and stress transformation rule. The result is

$$\sigma_{a_1}/\sigma_a = (Q_{11}\bar{S}_{11}+Q_{12}\bar{S}_{12})\cos^2\phi+(Q_{12}\bar{S}_{11}+Q_{22}\bar{S}_{12})\sin^2\phi + 2(Q_{16}\bar{S}_{11}+Q_{26}\bar{S}_{12})\sin\phi\cos\phi \tag{27}$$

where σ_{a_1} denotes the average stress of σ_1 over a characteristic length a_1, and σ_a has been given in Eq. (23)

In this model, the characteristic length can be considered as a two dimensional parameter because the stress at each point along the characteristic length is taken into account. Therefore, in this model the Strength Reduction Factor becomes:

$$\text{SRF} = \frac{\text{FPF or FF (Notched) at } (0,a_1)}{\text{FPF or FF (Unnotched)}}$$

Minimum Strength Model (MS). The two dimensional exact elasticity solution, Eq. (1-16), is incorporated with the present model. Many selected points on a characteristic curve (dotted line in Fig. 2) were examined to see if they satisfy the failure condition (FPF or FF) of Eq. (17).

The characteristic curve of an elliptical opening is described by:

$$\frac{x^2}{(a+b_0)} + \frac{y^2}{(b+b_0)} = 1 \qquad (28)$$

where b_0 is the characteristic length. If any point of Eq. (28) for any lamina satisfies the failure condition, Eq. (17), the whole laminate would fail. Strength Reduction Factor can be written as:

$$SRF = \frac{\text{FPF or FF (Notched) at the characteristic curve of Eq. (28)}}{\text{FPF or FF (Unnotched)}}$$

Above models can therefore be utilized to calculate the strength of notched composite laminate with a reinforcement. As an example, using minimum strength model the strength of laminate with an inclusion was predicted analytically for a CFRP T300/5208 $[0/\pm45/90]_s$ laminate under tensile loading as shown in Fig. 5. It can be seen here that there is considerable improvement in the notched strength of this laminate especially with aluminum inclusion. However, there are no experimental verifications of these models. Hence the present study was undertaken.

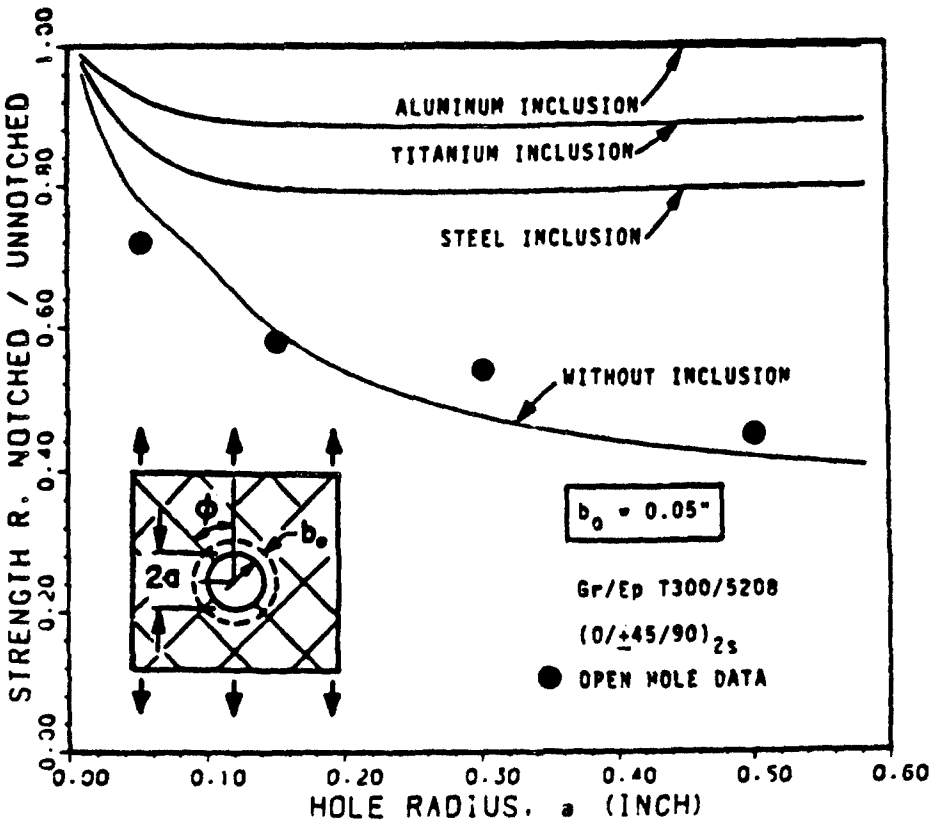

Fig. 5. Strength Reduction Factor of GR/EP Laminate with an Open Hole, and Hole with Aluminum Inclusion and Steel Inclusion, from Ref. 12.

IV. Experimental Procedure

One of the objectives of the present study was to evaluate the strength reduction of a composite laminate with a reinforced hole. A test program was, therefore, designed to evaluate the effect of the following factors on the strength reduction.

1. Type of reinforcement - (a) adhesively bonded plug and (b) snug-fit (finger press fit) plug.
2. Material of reinforcement - (a) steel, (b) aluminum and (c) plexiglass.
3. Hole sizes - four different diameters - 0.1", 0.2", 0.4" and 0.6".
4. Loading type - (a) tension and (b) compression.

Further, the test program included the investigation of chronology of failure progression in these composite laminates with reinforced hole. All these tests were conducted at room temperature.

Material Selection and Specimen Preparation

The material selected for the present study was graphite/epoxy composite system used in aerospace structures.

Three panels (24"x24", 18"x24", 14"x18") were prepared from preprag using the standard curing process at same conditions. To make sure that these were free from defects, each panel was inspected by X-ray techniques. These panels

were of quasi-isotropic lay-up of $[0/\pm 45/90]_{2s}$. The nominal thickness was 0.08 inch.

To investigate the effect of material of reinforcement, three materials having different stiffness were used for inclusion as mentioned before. Steel has much higher stiffness than base laminate. On the other hand, the stiffness of aluminum is almost same as of quasi-isotropic GR/EP composite and plexiglass has much lower stiffness than composite. Material properties for inclusions are shown in Table I.

Table I

Material Properties of GR/EP and Reinforcement

Parameters	AS4/3501-6 (10^6 psi)	Steel (10^6 psi)	Aluminum (10^6 psi)	Plexiglass (10^5 psi)
Longitudinal modulus, E_{11}	20.87	30	10	4.5
Transverse modulus, E_{22}	1.72	30	10	4.5
Shear modulus, G_{12}	0.97	11.63	3.85	1.67
Poisson's ratio, ν_{12}	0.326	0.29	0.30	0.35

The absolute minimum number of test specimens necessary to produce meaningful results was considered to be three due to the statistical failure nature of composites. The ultimate strength was therefore based on three ostensibly identical tests. At least two specimens from each test conditions were strain gaged to measure strain-to-failure

for the laminate. For each case one set of specimen was investigated by X-ray approximately at 35, 50, 70, 88, and 95% of failure load to study failure mechanism. The number of test specimens and conditions tested are shown in Table II.

Table II

Test Plan

Boundary Condition	Reinforcement Material	Loading	Hole Diameter				Total
			0.1"	0.2"	0.4"	0.6"	
Unbonded	Aluminum	Tension	3	3	3	3	12
		Compression	3	3	3	3	12
	Plexiglass	Tension	3	3	3	3	12
		Compression	3	3	3	3	12
	Steel	Tension	3	3	3	3	12
		Compression	3	3	3	3	12
Bonded	Aluminum	Tension	3	3	3	3	12
	Plexiglass	Tension	3	3	3	3	12
	Steel	Tension	3	3	3	3	12
Total			27	27	27	27	108

All specimens were cut by a diamond saw and end tab were attached. Gage length of tension specimen was selected as 6" to exclude edge effect, but for compression it was selected as 4" to prevent buckling of specimen. Typical specimen dimensions (both tension and compression) are shown

in Fig. 6 with the location of strain gages. The end tab material was 1/16" thickness glass/epoxy. These end tabs were bonded to the specimen with a bonding solution of general purpose epoxy, which contained 50/50 by weight mixture of Epon 828 and Versamid 140 respectively. After attaching end tabs, these specimens were heat treated at 250°F for two hours to insure complete bonding.

The holes in specimen were drilled by a carbide tipped drill at the specimen center. Drilling the hole in each specimen was started by using a small drill, with additional aluminum plate attachment on both top and bottom surface of specimen to prevent burs. The hole was then carefully enlarged to its final dimensions.

The reinforcing plug was made by using an automatic turning machine with ceramic tipped cutting tool by setting low feeding and high turning speed (to get very fine and uniform surface). To make the maximum contact between plug and hole, and for convenience of handling (especially during bonding), the plug length was selected equal to 4 times the thickness of laminate for both of tension and compression test specimen. In this case the stress distribution of composite laminate around the hole becomes more complicate due to the extended length of the plug. However, based on the assumption that the stress through the thickness are uniform as in the solution of Seika and Ishii (25), the stress concentration becomes less than the case of same length plug as the thickness of laminate.

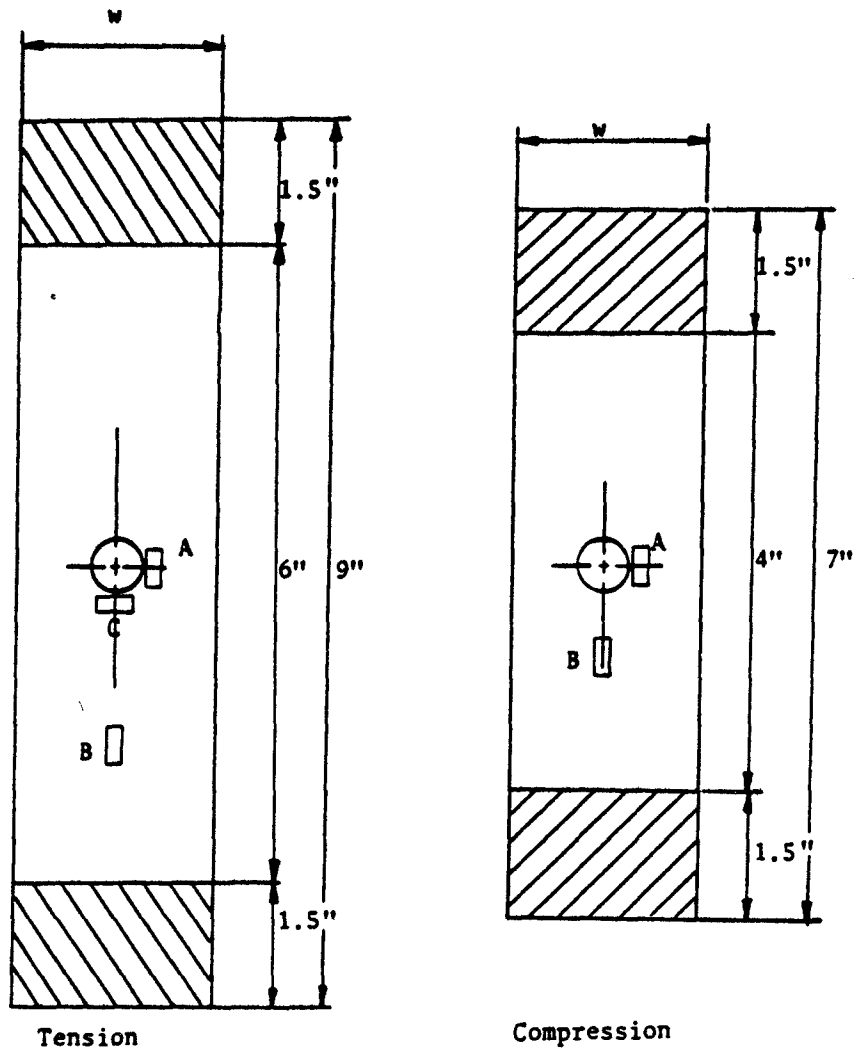

Fig. 6. Specimen Configuration (w = 1.0" for Hole Diameters 0.1" and 0.2", and w = 1.5" for Hole Diameters 0.4" and 0.6").

During preliminary tests, three types of structural adhesives - EA9302 (Hysol), FM-1000, Epoxy Resin - were employed to find the best adhesive. These tests showed that although none of these adhesives were good enough to maintain their strength up to the failure of tested laminates, however, EA9302 (Hysol) turned out to be the best adhesives out of three. The properties of EA9302 are shown in Table III.

Table III

Properties of Structural Adhesive EA9302 (Hysol)

Product designation	EA9302 NA
Description	Thixotropic paste with liquid curing agent.
Special properties	High shear and peel strength from -67°F to 200°F.
Recommended cure	3-5 days at 77°F
Pot life	25-30 minutes (250 grams at 77°F)
Self life	1 year at 77°F
Service temperature	-67°F to 225°F

The bonding procedure consisted of several steps. First of all, both surfaces of plug and hole were roughened with sand paper and then, scribed with sharp knife edge in the direction of 45°. Thereafter surface preparation was done in the following manner, for both of plug and inside of laminate hole.

1) Vapor degrease with alkaline cleaner, rinse with distilled water, and dry surface.

2) Immerse in sodium dichromate sulfuric acid solution for 10 to 13 minutes at 145° to 155°F. This solution is made as follows:

Sodium Dichromate
FED O-S-595A ----------28.5 grams
Sulfuric Acid
FED O-A-115, Class A, Grade 2 ----------285.0 grams
Water ----------to make 1 liter.

3) Spray rinse with cool distilled water (at or below 75°F).

Bonding was conducted at the laboratory which had constant moisture (45%) and temperature (75°F). The ratio of paste adhesive and curing agent (fluid) was 100 to 22 by weight. Using wood stirring rod, the adhesive (which has high viscosity) was put first in an aluminum cup, then curing agent was added after weighing separately. Then both were mixed together thoroughly. This mixed adhesive was applied on the plug surface and inside of laminate hole. After spreading the adhesives on both surface uniformly, using tweezers the plug was carefully put inside of the hole. Then, holding the top and bottom of the plug, it was moved backward and forward several times to spread adhesive evenly between hole and plug. At least five days were allowed for curing the adhesive by placing the bonded

specimen in the same room with controlled moisture and temperature.

For the case of bonding, 0.004" clearance between plug and hole was selected to obtain a good bondline between plug and composite. But for unbonded case, the plug was made of almost same size (less than 0.001" clearance) as of hole, so it can be fit with hard finger pressure, and have the maximum contact with hole but not damage the inside wall of the hole. To prevent moisture and temperature degradation of specimen, every specimen was preserved in the desiccator which was located in constant temperaturized room.

Test Procedure

Instron floor model TT-D with the load capacity of 20000 lb was used for both tension and compression test, see Fig. 7. For both tension and compression tests, same "GR" load cell (capacity = 20000 lb) and 0.02 inches per minute crosshead speed were used. During the test, the stress-strain curves as well as load-crosshead displacement relations were recorded.

For tension test Micro Measurement 120 and 350 ohm strain gages having gage length of 62, 75 and 250 milliinch were used to measure the strain of laminate as well as the strain near of the hole. The location of these gages on a specimen are shown in Fig. 6. Strain gage "B" (250 milliinch 120 ohm) was used to measure the strain in the laminate away from the hole while strain gages, "A" and "C",

both 75 milliinch 350 ohm with 0.4" and 0.6" hole sizes, and 62 milliinch 350 ohm with 0.1" and 0.2" hole sizes were used to measure the strain near the hole.

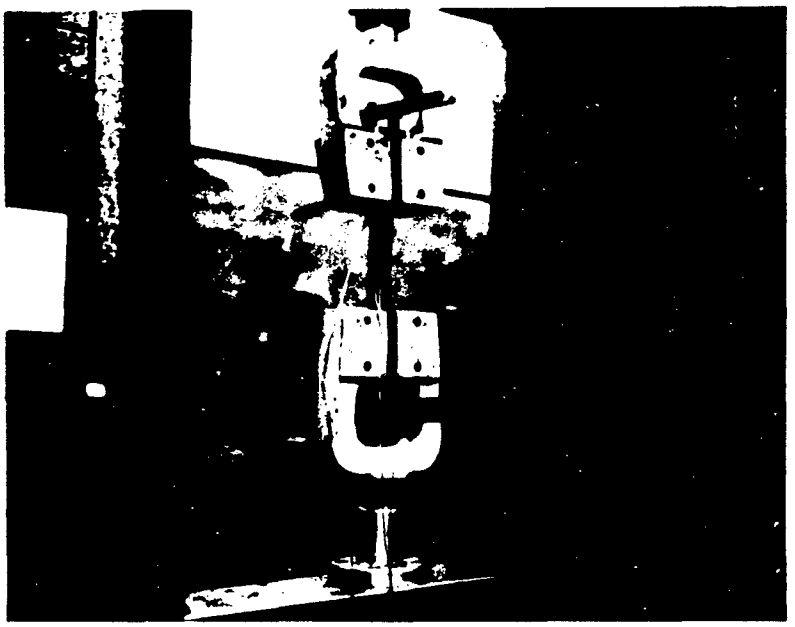

Fig. 7. Tension Test With Strain Gaged Specimen.

For compression test, different type of grips were used, and another attachment panel was made to hold that grip as shown in Fig. 8. To prevent buckling of specimen, anti-buckling fixture was used with C-clamp as shown in Fig. 9. To measure the strain response, two strain gages - "A" and "B" - were used that had same sizes as in tension case, and their locations on the specimen are also shown in Fig. 6.

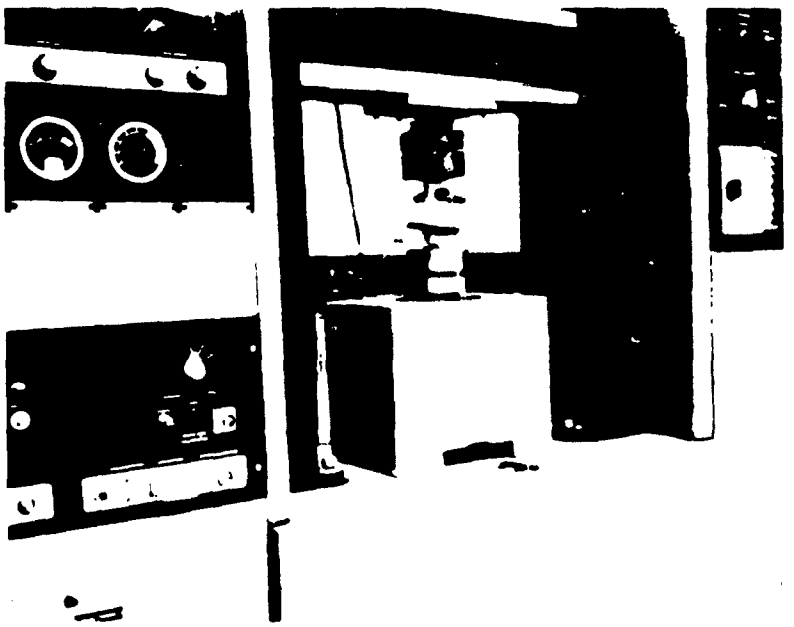

Fig. 8. Compression Test Equipment.

The failure mechanism was investigated by using microscope and X-ray technique. For each case of different size and inclusion, one specimen was loaded incrementally up to failure at a certain amount of interval. For the bonded case, the specimen was taken out from machine after increasing each interval of load. Using a microscope (50X to 500X magnification ratio) the surface of specimen near the bondline was inspected to find the nature and location of the damage, if any. Thereafter, the specimen was taken for X-ray inspection to find the overall view of damage initiation and progression over the whole specimen. For the specimen with snug-fitted plug, the same number of specimens were used to study the failure mechanism. But in this case X-ray technique was only employed at each interval of load.

The results of all these tests will be presented and discussed in the next chapter.

Fig. 9. Compression Test Specimen and Anti-buckling Support

V. Results and Discussions

In the first series of experiments, tension and compression tests of unnotched and open hole specimens were conducted to develop the data base for comparison with the results of reinforced hole specimens. Three identical tests were done for each case and the summary of these tests results are given in Table IV.

Experimental work was, thereafter, concentrated on the case where specimen had bonded reinforcement under tension loading. These tests showed that the improvement in ultimate strength of reinforced hole laminate with respect to open hole specimen was almost negligible. The reason for this was that adhesive was too weak to endure the failure load of specimen as it will be discussed in detail in a subsequent subsection. Then, the emphasis was moved towards the testing of laminate with unbonded reinforcement.

In each test, the complete history of load versus displacement was recorded. Three typical load-displacement curves for tension and compression cases are shown in Figs. 10 through 12. As it can be seen from these, the stress-strain relation away from the hole was linear and failure occurred in the brittle manner in all cases. The strain near the side of hole (A) showed quite linear response up to failure. However, the amount of strain (A) was more than twice of the strain away from the hole (B) at the same load. These strain responses were almost same for all different

inclusions and boundary conditions. When the hole size was smaller, the slope of strain response between strain gage at locations (A) and (B) showed less difference than in comparison to the case with the large hole.

Table IV

Notched Strength of Specimen with Open Hole

Condition	Hole Size (inch)	Width (inch)	Average Notched Strength (psi)	Unnotched Strength (psi)	$\frac{\sigma_n}{\sigma_0}$
Tension	0.1	1.0	72435	97931	0.739
	0.2	1.0	54000		0.551
	0.4	1.5	50430		0.515
	0.6	1.5	48965		0.500
Compression	0.1	1.0	66667	86890	0.767
	0.2	1.0	53205		0.612
	0.4	1.5	46322		0.533
	0.6	1.5	43589		0.502

The typical failed specimens for both tension and compression are shown in Fig. 13 and 14, respectively. Generally the tension failure occurred approximately at $\pm$45 degree direction with the main load axis. However, the compression failure occurred at almost 90 degree direction with respect to the load axis. These results are discussed in detail for each case in the following.

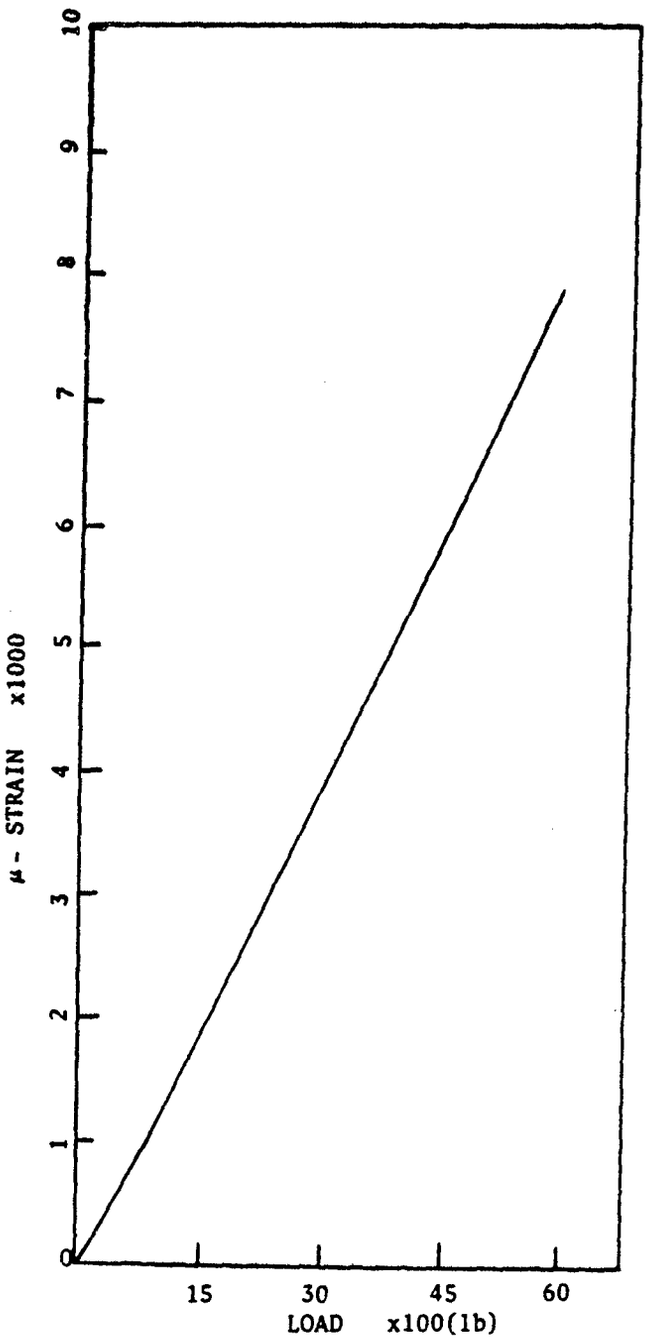

Fig. 10. Typical Strain Response of Far Field Strain Gage (B) in Tension Test (0.2" Aluminum reinforcement, Bonded).

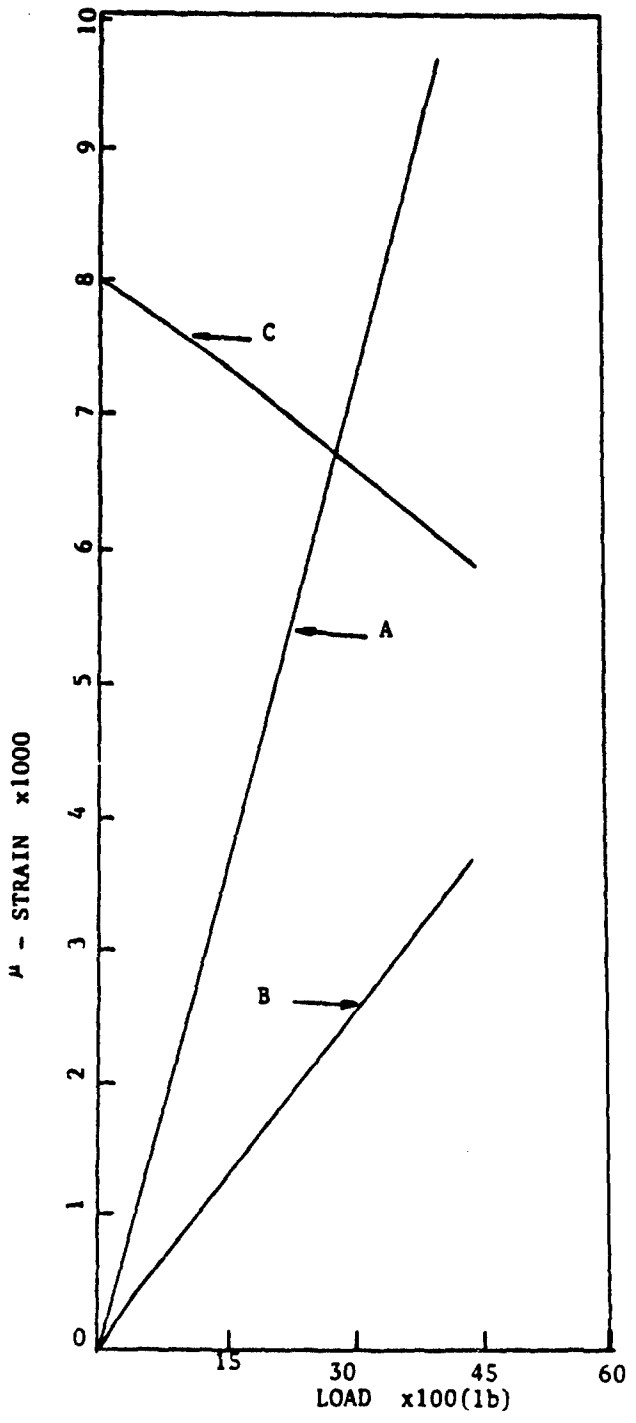

Fig. 11. Typical Strain Responses for Tension Test (9.6" Plexiglass Bonded Reinforcement up to 90% Load).

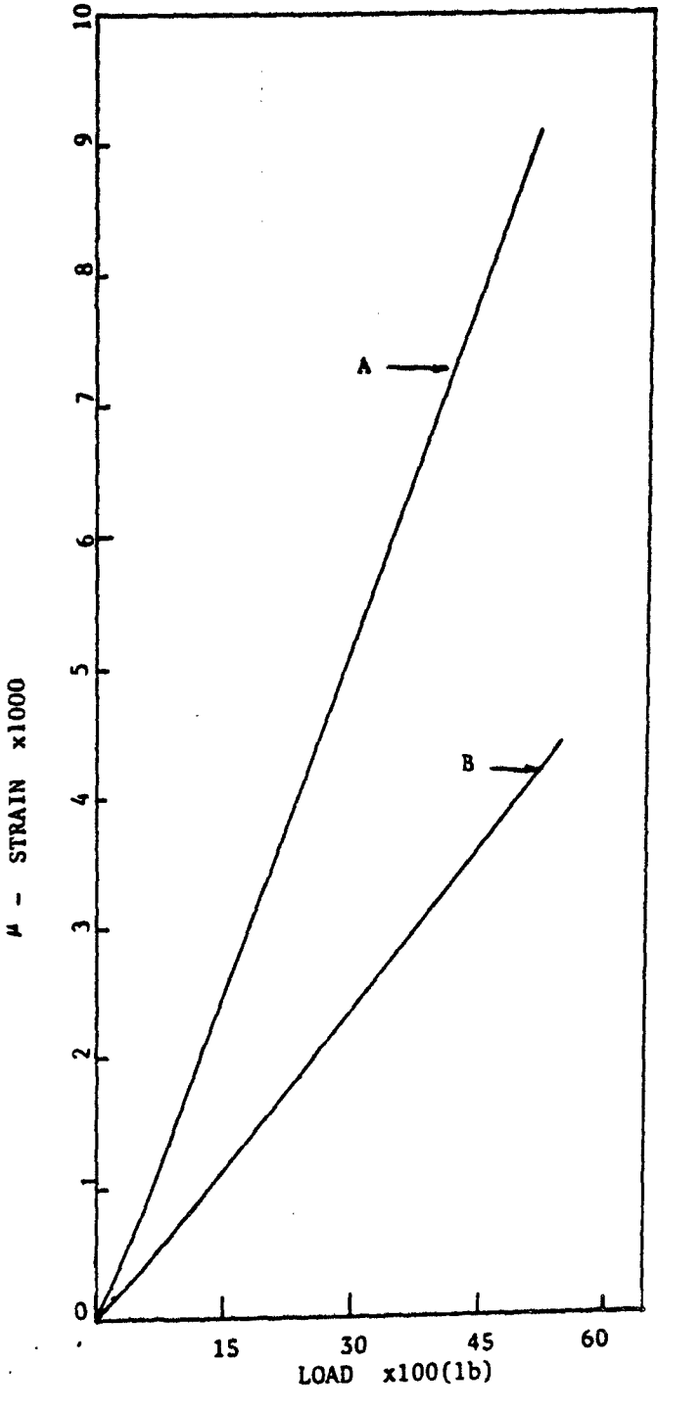

Fig. 12. Typical Strain Responses for Compression Test (0.6" Plexiglass Unbonded, up to 90% of Failure Load).

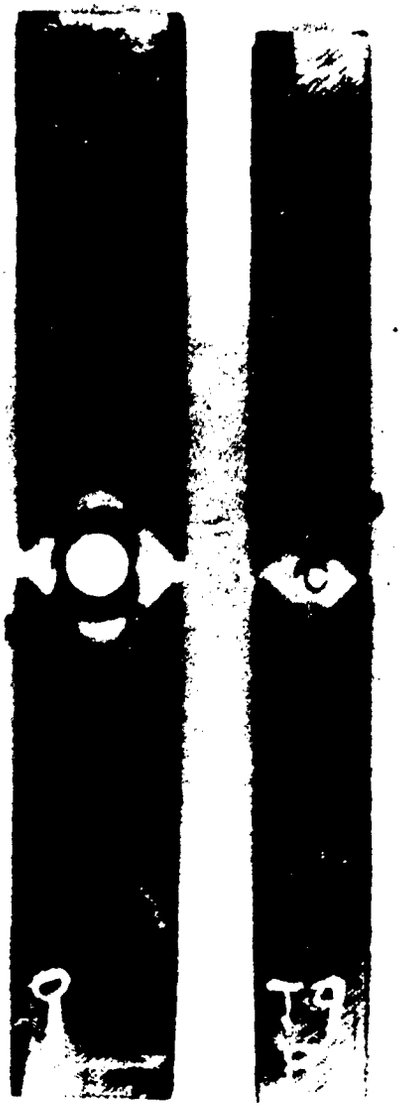

Fig. 13. Typical Failure Mode of Tension Test (Left: 0.6" Aluminum Bonded, Right: 0.2" Aluminum Unbonded).

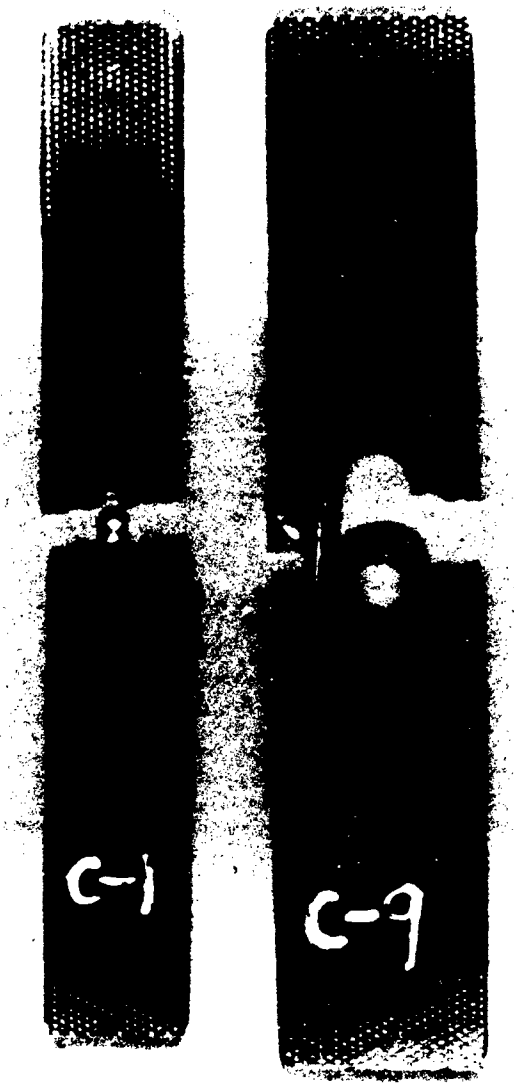

Fig. 14. Typical Failure Mode of Compression Test (Left 0.2" Aluminum Unbonded, Right: 0.6" Plexiglass Unbonded).

Bonded Specimen

The results from this series of experiments are discussed in two parts; (1) change in strength due to the bonded reinforcement, and (2) the progression of failure process.

Test Results. Three different types of commonly used aerospace structural adhesives were used during preliminary tests with 0.2" hole size. The EA9302 (Hysol) was first employed after doing thorough surface treatment as mentioned before. The measured strength were compared with its counterpart from open hole as shown in Table V. As it can be noticed from this table, the increase of the ultimate strength was not as much as expected. Therefore, two other aerospace adhesives, FM-1000 and Epoxy-resin, were used to improve the ultimate strength.

The FM-1000 is a film type adhesive especially made for aerospace structure. Although it can stretch with the hand into a thin layer, it was very hard tc wrap around of the plug and thereafter fit it into the inside of the hole. Thus, it was very difficult to handle during bonding. Epoxy Resin was then employed for few cases, but the results from these two adhesives showed no improvement, as can be seen in Table V.

On the post-mortem examination of specimens, it was noticed that in most cases failure initiated at the interfaces. These interfaces can be either between plug and

adhesive or between glue and composite laminate. By changing several kinds of surface preparation methods (using different grid sizes of sand paper, different type of scratching method, etc). the author tried to improve the bonding between the plug and specimen. But the test results from these showed no improvement. These preliminary tests, thus, showed that EA9302 was, in general, better adhesive than in comparison to FM-1000 and Epoxy-resin.

Table V

Preliminary Test Results with 0.2" diameter Aluminum plug

Adhesive	Clearance (inch)	Ultimate Strength (psi)	$\frac{\sigma_n}{\sigma_0}$	Increase from open hole (%)
EA9302 (HYSOL)	0.001	51067 (psi)	0.555	0.680
	0.001	50070	0.590	7.551
	0.002	57146	0.500	5.830
	0.003	60695	0.622	12.901
	0.004	50971	0.602	9.209
	0.007	61011	0.626	10.600
	0.010	57012	0.502	5.628
	0.010	53948	0.551	0.001
	0.015	56096	0.573	3.891
FM-1000	0.003	53205	0.543	-1.470
	0.005	54700	0.550	1.302
	0.010	55556	0.567	2.806
	0.015	55550	0.566	2.804
Epoxy-Resin	0.001	54965	0.561	1.789
	0.002	52866	0.540	-2.058
	0.004	48461	0.495	-10.261
	0.0006	49679	0.507	-8.008

After selecting EA3902 (Hysol) adhesive, several tests were run to investigate the effect of bondline thickness (i.e. clearance between hole and plug). These tests results are also shown in Table V. From these preliminary results as well as from bonding experience, the clearance of 0.004" to 0.005" was selected for the final series of tests involving four hole sizes. Also, plexiglass and steel was used as reinforcement material to investigate the effect of plug material. All these results are given in Table VI.

To compare the results of each reinforcement case with that of open hole directly, these are plotted in Figs. 15 (a) through 15 (d). In these figures each symbol indicates the average value of three test results.

Table VI

Tension Test Results (bonded reinforcement)

No	Inclusion	Hole Size	Ultimate Strength (psi)	$\frac{\sigma_n}{\sigma_0}$	Increase from open hole (%)	Average Increase (%)
1	Aluminum	0.1	68590	0.701	-5.310	-0.423
2			74205	0.758	2.510	
3			73545	0.751	1.520	
4		0.2	53205	0.543	-1.470	3.351
5			60235	0.615	11.551	
6			53895	0.550	-0.261	
7		0.4	52990	0.541	5.079	5.470
8			53450	0.546	6.001	
9			53125	0.543	5.340	
10		0.6	41880	0.428	-14.470	-3.371
11			49541	0.506	1.181	
12			50520	0.516	3.179	
13	Plexi-glass	0.1	69231	0.707	-4.423	-1.352
14			71981	0.735	-0.629	
15			73150	0.747	0.997	
16		0.2	57051	0.583	5.648	5.650
17			55769	0.570	3.280	
18			58333	0.596	8.019	
19		0.4	51282	0.524	1.690	-0.119
20			50256	0.513	-0.345	
21			49573	0.506	-1.701	
22		0.6	38461	0.393	-21.451	-11.561
23			44444	0.454	-9.230	
24			47008	0.480	-4.001	
25	Steel	0.1	69230	0.707	-4.425	-4.129
26			64103	0.655	-11.503	
27			75000	0.766	3.541	
28		0.2	57051	0.583	5.648	1.297
29			52564	0.537	-2.695	
30			54487	0.556	0.902	
31		0.4	50427	0.515	-0.006	0.842
32			48718	0.498	-3.395	
33			53419	0.546	5.927	
34		0.6	44017	0.449	-10.105	-4.778
35			46153	0.471	-5.740	
36			49572	0.506	1.242	

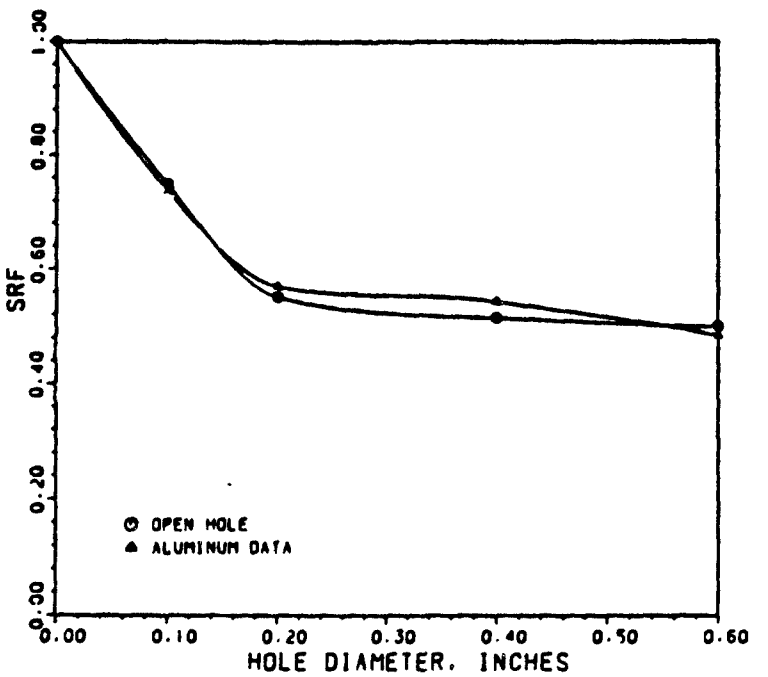

Fig. 15 (a). Comparison of Strength Reduction Factor (SRF) of the Open Hole versus Bonded Reinforcement (Aluminum).

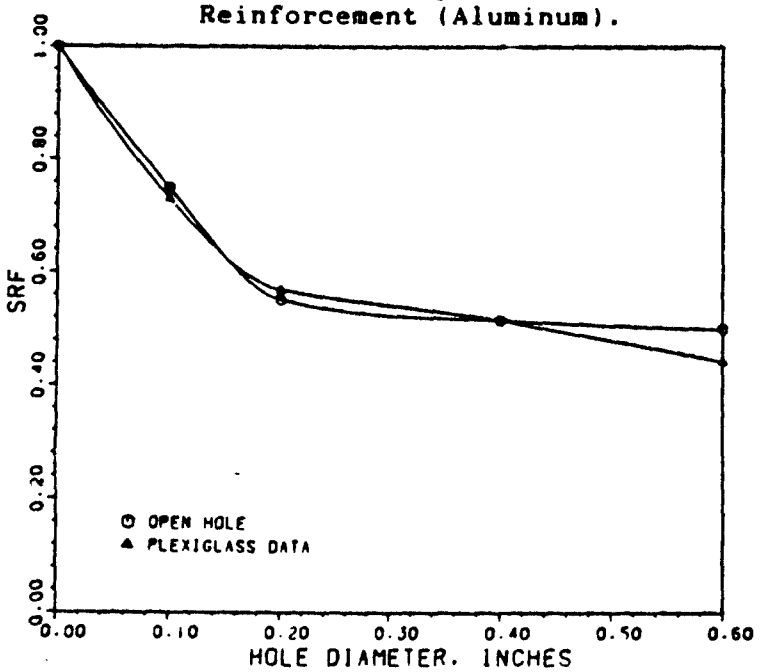

Fig. 15 (b). Comparison of Strength Reduction Factor (SRF) of the Open Hole versus Bonded Reinforcement (plexiglass)

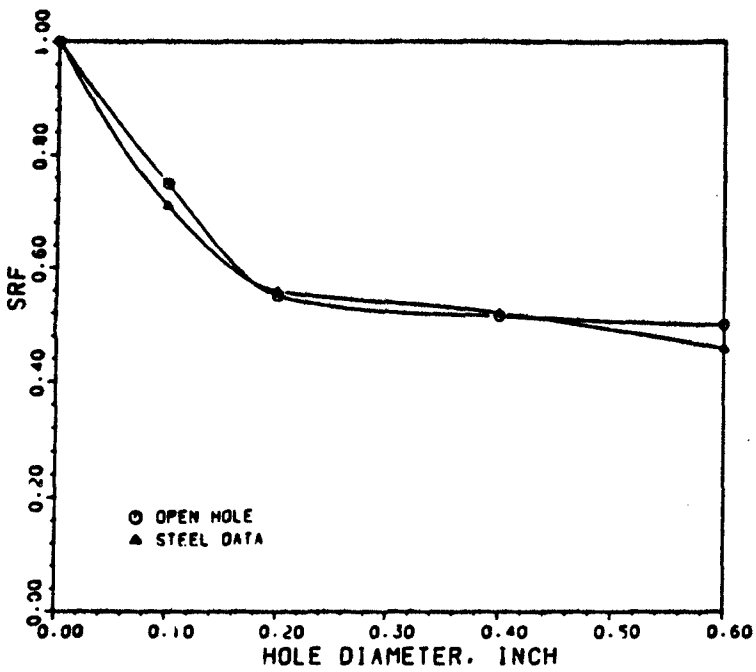

Fig. 15 (c). Comparison of Strength Reduction Factor (SRF) of the Open Hole versus Bonded Reinforcement (steel).

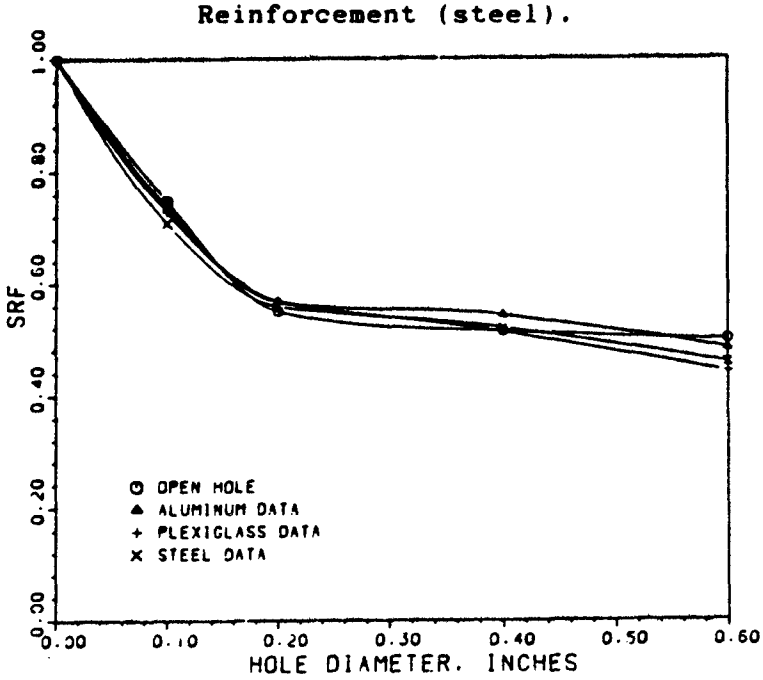

Fig. 15 (d). Comparison of Strength Reduction Factor (SRF) of the Open Hole versus Three Bonded Reinforcements.

These results as given in Fig. 15, clearly shows that there was no improvement due to bonded reinforcement for any hole size and for any plug material contrary to the expected increase in strength. To investigate the reason for this, the initiation and progression of damage in these tests were examined and is discussed next.

Failure Mechanism Analysis. As mentioned previously, to determine the whole chronology of failure mechanism, few specimens were loaded and unloaded at increment of certain percentage of failure load. And at each interval, these specimens were inspected by microscope and x-ray technique.

The initiation of crack in bondline was clearly seen by using microscope. Approximately at 88 to 91% of the failure load, bondline failure started from the top and bottom portion of the reinforcement as depicted in Fig. 16. Typical magnified pictures of these area are shown in Figs. 17 through 19. In these pictures, the white portion is reinforcement, and the gray part and darker portion are adhesive and composite laminate, respectively.

In almost all the cases, failure initiated at the interface, either between adhesive and inclusion (Fig. 17) or between adhesive and composite laminate (Fig. 18). Once the crack initiated, it grew usually criss-crossing from one interface to the other (Fig. 19) when the load was increased further, and from that moment the plug was separated from the hole. Once the separation occurred, the reinforcement

was no more useful. Thereafter, the catastropic failure occurred immediately.

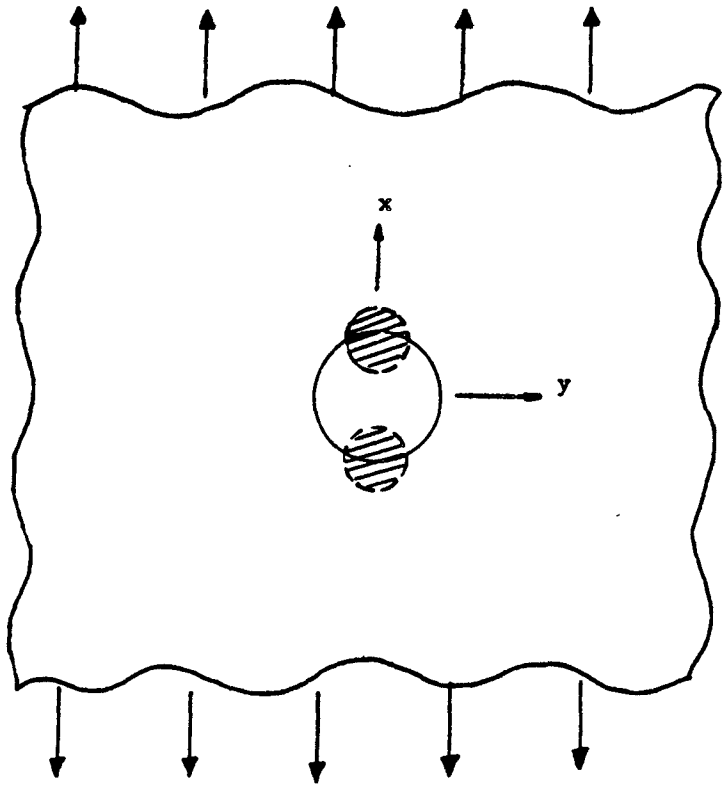

Fig. 16. The Position of Bondline Failure Initiation.

Fig. 17. Failure Initiation (a) (X100, 0.6" Plexiglass)

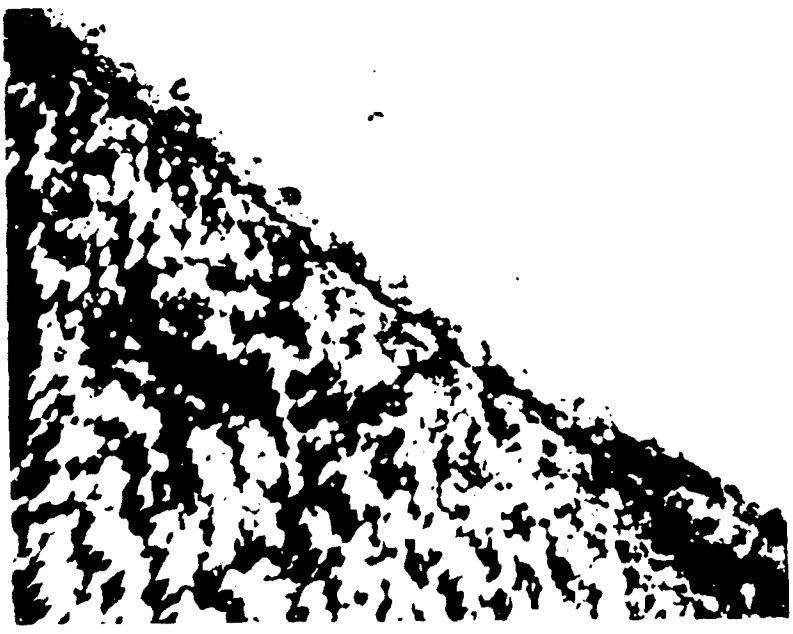

Fig. 18. Failure Initiation (b) (X200, 0.6" Aluminum)

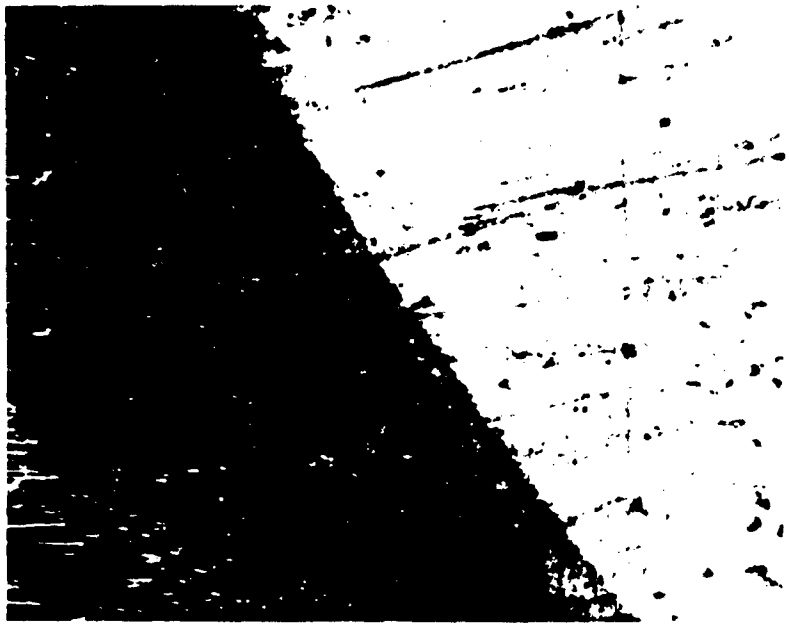

Fig. 19. Failure Initiation (c) (X100, 0.4" Aluminum)

The results from X-ray inspection were shown at Figs. 20 to 24. In these pictures the dark gray portion near of the hole indicates adhesives that were smeared out from the hole during the curring process, and the black lines starting from both sides of the hole are strain gage wires.

As can be seen from Fig. 20, approximately up to 33% of failure load, no failure was observed. After increasing the load to 50% of failure load, 90^0 matrix started failing at several places of the specimen (Fig. 21). At the next increment of load (70% of ultimate strength), 90 matrix failure occurred a lot more especially near the hole area (Fig. 22).

Fig. 20. X-Ray Results of Bonded Tension Test (33% load). (Left: 0.2" Aluminum, Right: 0.4" Aluminum)

Fig. 21. X-Ray Results of Bonded Tension Test (50% load, Left: 0.2" Aluminum, Right: 0.4" Aluminum.)

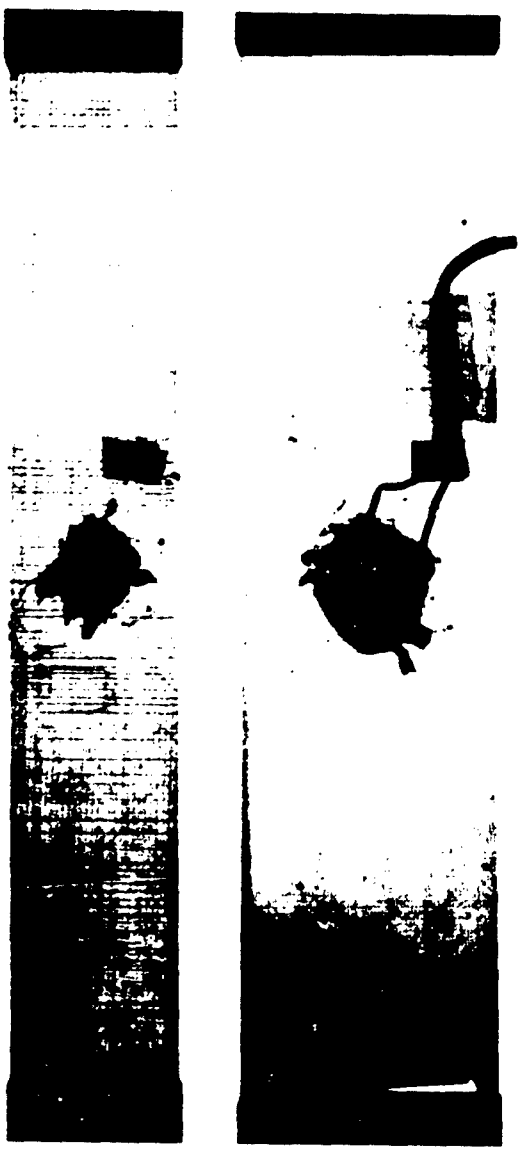

Fig. 22. X-Ray Results of Bonded Tension Test (70% load, Left: 0.2" Aluminum, Right: 0.4" Aluminum.)

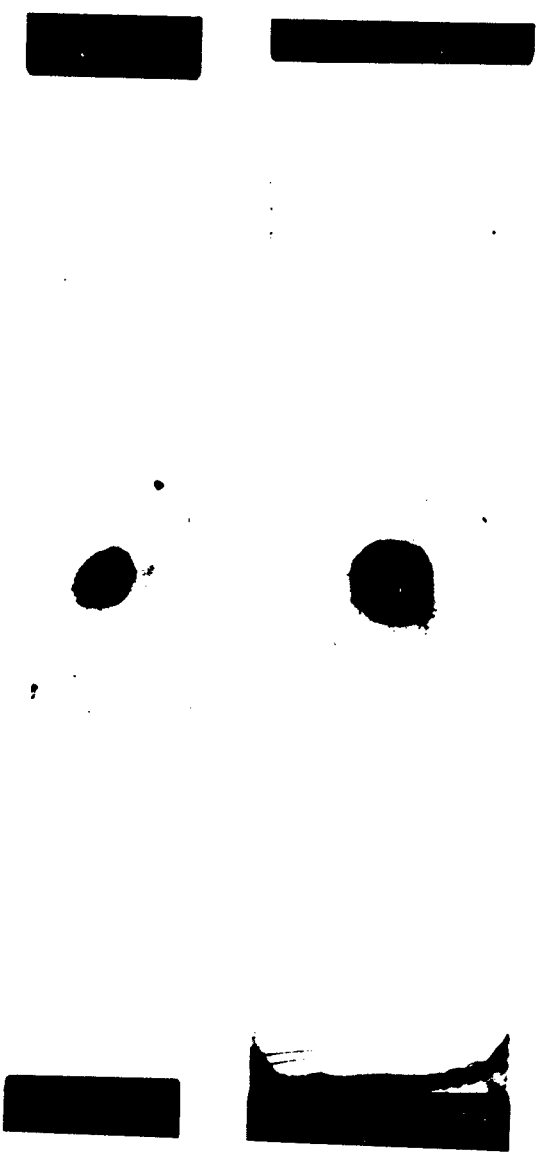

Fig. 23. X-Ray Results of Bonded Tension Test (88% load, Left: 0.2" Aluminum, Right: 0.4" Aluminum.)

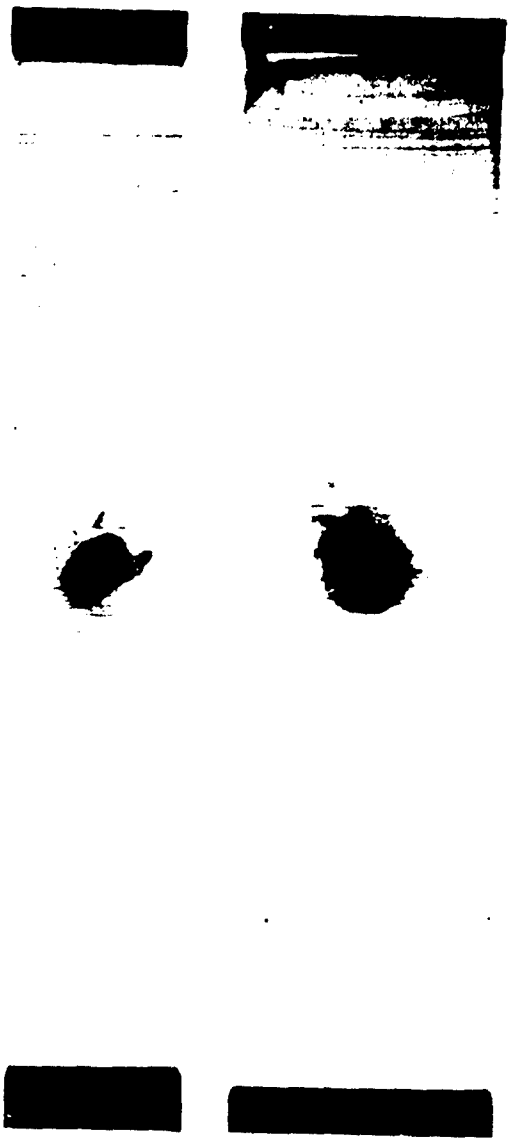

Fig. 24. X-Ray Results of Bonded Tension Test (95% load, Left: 0.2" Aluminum, Right: 0.4" Aluminum.)

At 88% of failure load, crack initiated in bondline as mentioned previously. And then, at about 95% of failure load, 90^{0} matrix failed almost everywhere in the specimen.

Through this investigation of failure mechanism X-ray results did not show about delamination as increase the load however, the magnified pictures taken from microscope showed clearly that failure occurred from bondline. Hence, the bonded reinforcement showed no improvement in the notch strength of laminate as mentioned before. It can be concluded that the full benefit of bonded reinforcement can not be realized until a proper bonding can be achieved. Author devoted a great amount of effort in this direction, but it is very difficult task due to limited space between hole and reinforcement.

Unbonded Reinforcement

The detailed experimental results for both tension and compression tests for unbonded reinforcement will be discussed in the following section.

Tension Test Results. During tension loading of reinforced composite laminate, it was very important to maintain the maximum contact between plug and surrounding hole throughout the whole load history. To do this it is necessary to make same size of plug as hole as possible, but not hurt the inside of the hole when plugging in. By the experience of several preliminary tests, it turned out that snug-fit clearance showed generally the maximum increase of ultimate strength. Here snug-fit means the condition that

the plug can be fitted with hard finger pressure and it can be moved inside the hole by finger pressure. The results of all these tension tests are shown in Table VII.

Table VII

Tension Test Results (unbonded plug)

No	Inclusion	Hole Size (inch)	Notched Strength (psi)	$\frac{\sigma_n}{\sigma_0}$	Increase from open hole (%)	Average Increase (%)
1	Aluminum	0.1	73366	0.749	1.285	1.178
2			72990	0.745	0.760	
3			73514	0.751	1.490	
4		0.2	57031	0.582	5.163	12.252
5			64192	0.655	18.874	
6			60625	0.619	12.269	
7		0.4	55417	0.566	9.889	11.102
8			55128	0.563	9.316	
9			57692	0.589	14.400	
10		0.6	51670	0.528	5.524	5.852
11			50830	0.519	3.809	
12			52991	0.541	8.222	
13	Plexi-glass	0.1	71794	0.733	-0.885	-0.582
14			73718	0.753	1.771	
15			70528	0.720	-2.633	
16		0.2	49572	0.506	-8.200	-1.604
17			55625	0.568	3.009	
18			54205	0.553	0.380	
19		0.4	51282	0.524	1.689	1.406
20			50427	0.515	-0.006	
21			51709	0.528	2.536	
22		0.6	44583	0.455	-8.949	-1.865
23			50854	0.519	3.589	
24			48717	0.497	-0.506	
25	Steel	0.1	70512	0.720	-2.632	0.008
26			74359	0.759	2.656	
27			74236	0.740	0.001	
28		0.2	58974	0.602	9.211	9.607
29			57692	0.589	6.837	
30			60897	0.622	12.772	
31		0.4	48718	0.498	-3.395	-0.570
32			52564	0.537	4.232	
33			49145	0.502	-2.548	
34		0.6	46154	0.471	-5.741	-2.250
35			49145	0.502	0.368	
36			48291	0.493	-1.37	

For the convenience of comparison, the results of each reinforcement versus open hole were plotted in Fig. 25 (a) through (d).

For aluminum reinforced case, there was about 5 to 12% improvement in the strength from open hole case for the hole diameter greater than 0.2". But, for 0.1" hole there was no such improvement. This may be due to very small amount of interaction between plug and composite laminate.

The results of plexiglass reinforcement showed no increase. Because the stiffness of plexiglass is too low in comparison to laminate, it did not respond to the load interaction inside of hole. In most case the plexiglass reinforcement fractured at same time when the laminate failed.

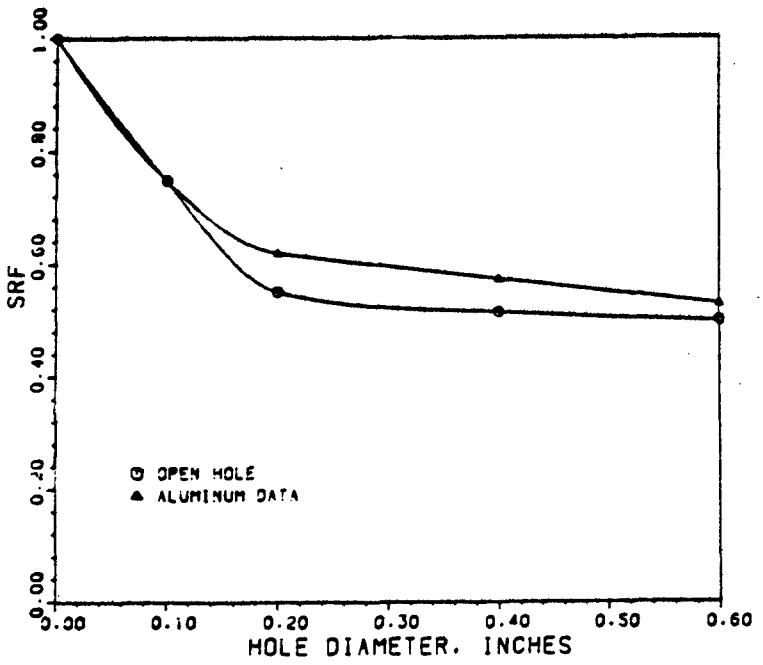

Fig. 25 (a). Comparison of SRF Between Unbonded Aluminum and Open Hole (Tension).

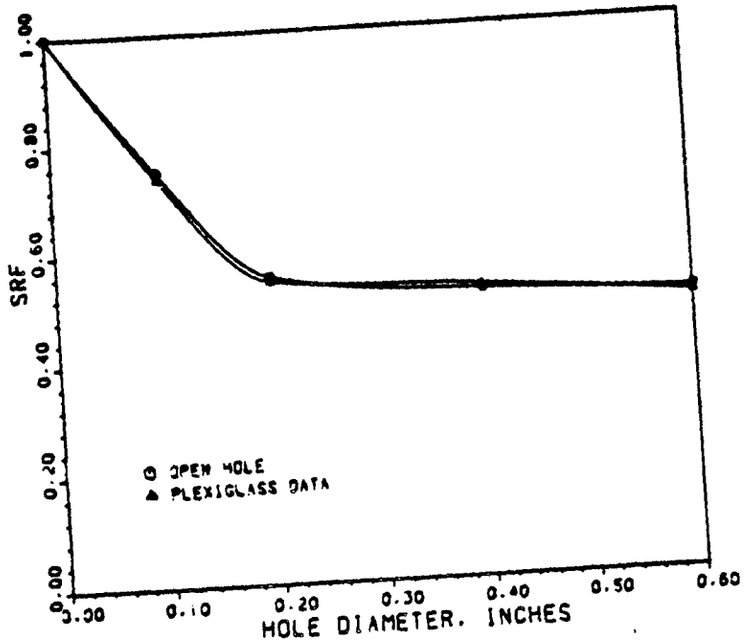

Fig. 25 (b). Comparison of SRF Between Unbonded Plexiglass Inclusion and Open Hole (Tension).

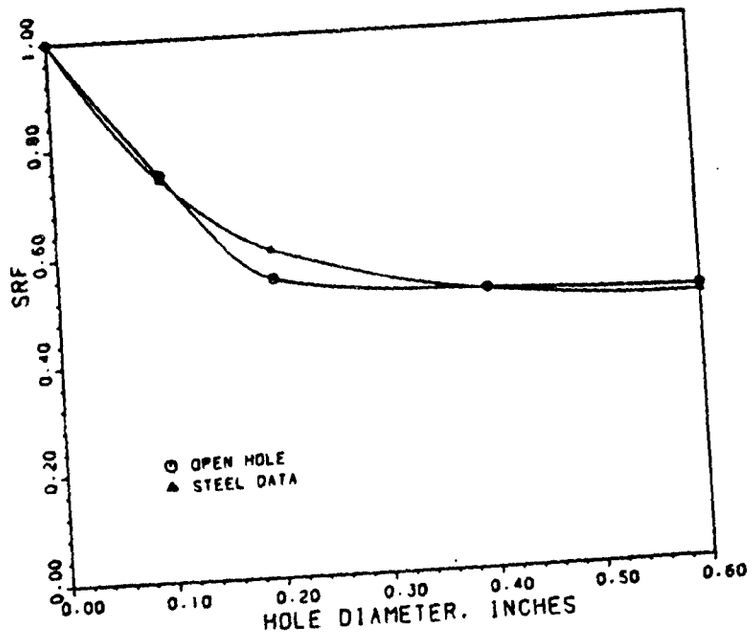

Fig. 25 (c). Comparison of SRF Between Unbonded Steel Inclusion and Open Hole (Tension).

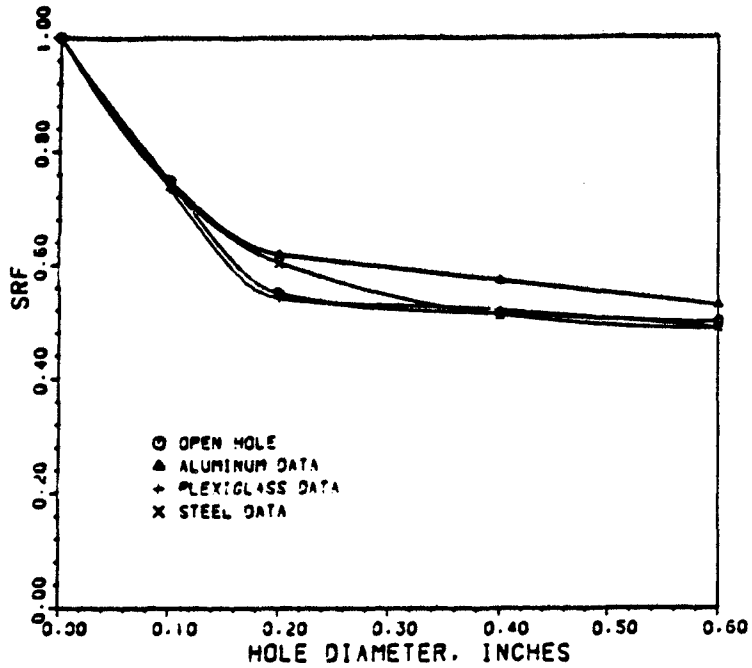

Fig. 25 (d). Comparison of SRF among all Unbonded Inclusions and Open Hole (Tension).

In case of steel inclusion, the results for 0.1" and 0.2" showed similar response as in case of aluminum, but for the case of larger hole, it showed less increase than aluminum. Since the stiffness of steel is much higher than that of composite, it did not follow the deformed shape of laminate hole with increase of the load.

In general, the aluminum reinforcement showed improvement of ultimate load relative to open hole. While, the steel and plexiglass inclusion showed no increase. This may be attributed to the difference in the moduli of laminate and reinforcement. As mentioned previously, aluminum has same Young's modulus as composite, plexiglass has far less than composite, and steel has greater than

composite. Thus it can be concluded that the reinforcement material should have the same Young's modulus as that base laminate for proper reinforcement.

Compression Test Results. The next series of experiment included the compression test with unbonded reinforcement. As in case of tension test, every inclusion was fitted with snug-fit clearance. The complete test results are shown in Table VIII and these results are plotted in Fig. 26 (a) through 26 (d) for comparison.

Table VIII

Compression Test Results (unbonded inclusion)

No	Inclusion	Hole Size (inch)	Notched Strength (psi)	$\frac{\sigma_n}{\sigma_0}$	Increase from open hole (%)	Average Increase (%)
1			74359	0.856	11.538	
2		0.1	76923	0.885	15.384	15.333
3			79487	0.915	19.230	
4			75461	0.871	42.269	
5		0.2	69230	0.797	30.119	36.546
6	Aluminum		73077	0.841	37.350	
7			64957	0.748	40.229	
8		0.4	68376	0.787	47.610	42.074
9			64102	0.738	38.383	
10			61583	0.709	41.281	
11		0.6	65812	0.757	50.981	48.320
12			66667	0.767	52.669	
13			70513	0.812	5.769	
14		0.1	65385	0.752	-1.923	3.486
15			71795	0.826	7.692	
16			65384	0.752	22.891	
17	Plexi-	0.2	62820	0.723	18.072	18.072
18	glass		60256	0.694	13.253	
19			54700	0.629	18.086	
20		0.4	52136	0.600	12.551	13.782
21			51282	0.590	10.708	
22			49572	0.571	13.726	
23		0.6	50427	0.580	15.687	15.687
24			51282	0.590	17.649	
25			80769	0.930	21.153	
26		0.1	78205	0.900	17.307	17.948
27			76923	0.885	15.384	
28			70512	0.812	32.529	
29		0.2	72436	0.834	36.145	32.129
30	Steel		67949	0.782	27.712	
31			66239	0.762	43.000	
32		0.4	67521	0.777	45.764	39.921
33			60684	0.698	31.000	
34			64102	0.738	47.060	
35		0.6	64957	0.748	49.022	46.081
36			61966	0.713	42.160	

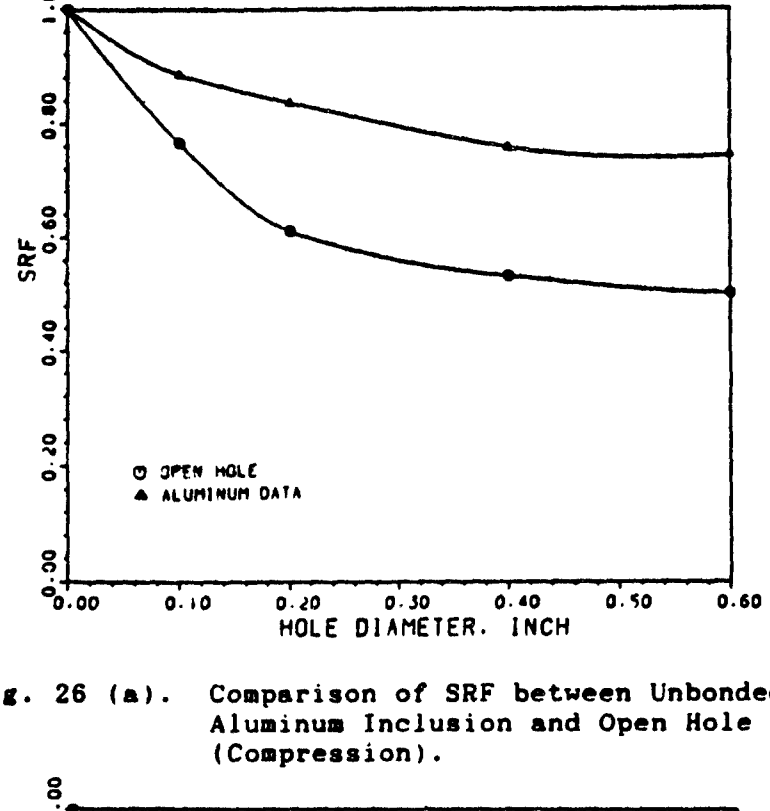

Fig. 26 (a). Comparison of SRF between Unbonded Aluminum Inclusion and Open Hole (Compression).

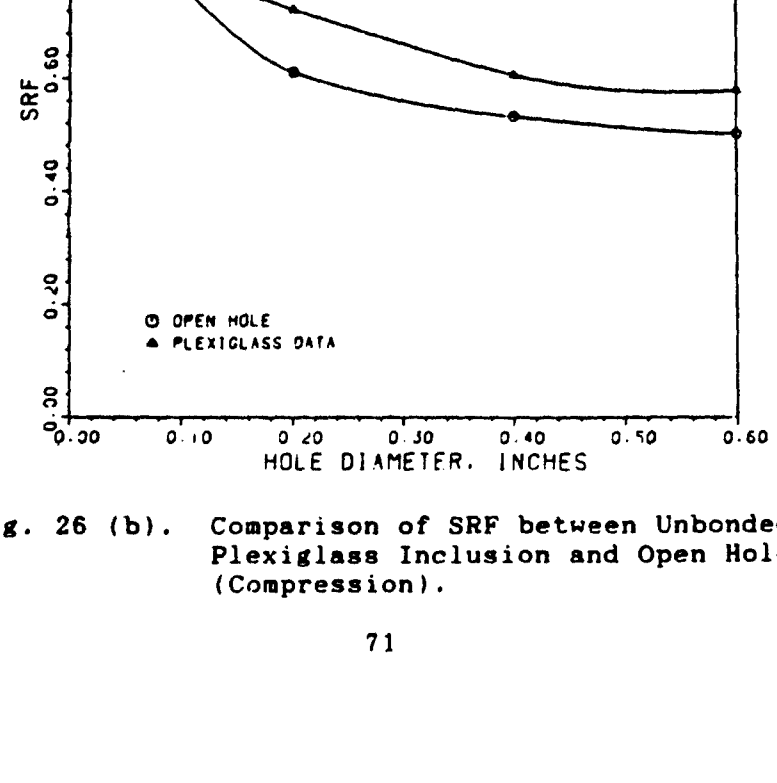

Fig. 26 (b). Comparison of SRF between Unbonded Plexiglass Inclusion and Open Hole (Compression).

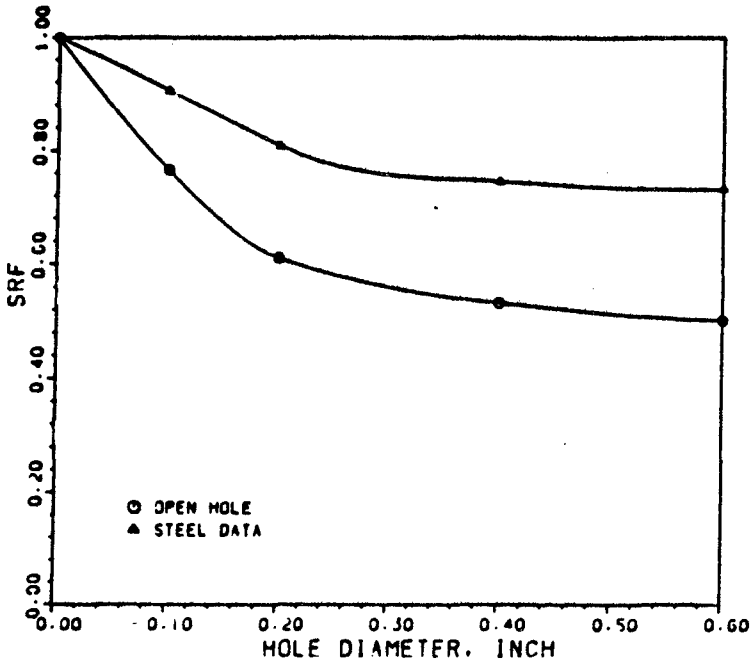

Fig. 26 (c). Comparison of SRF between Unbonded Steel Inclusion and Open Hole (Compression),

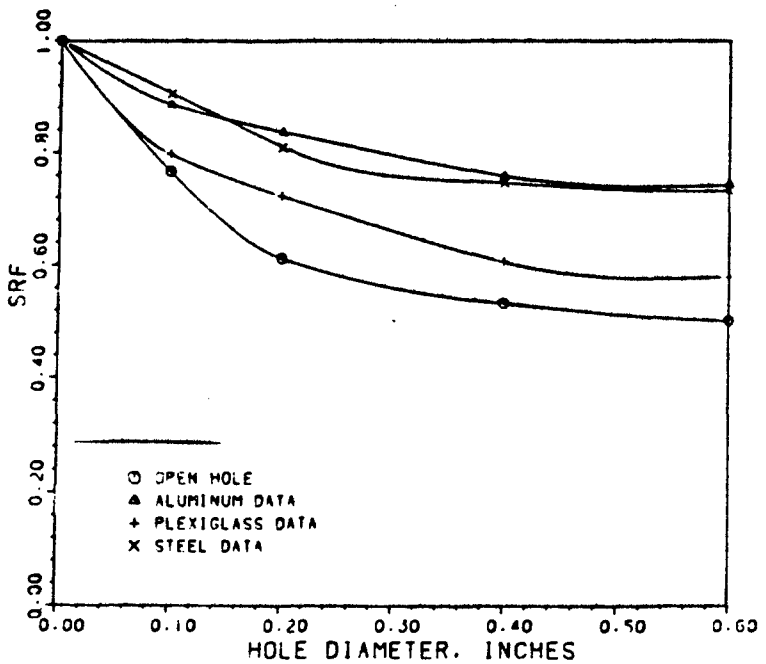

Fig. 26 (d). Comparison of SRF among All Unbonded Inclusions and Open Hole (Compression).

During compression test also, as in tension case, aluminum showed largest amount of improvement. For 0.1" diameter, as mentioned before the reinforcing area was very small, thus the improvement was relatively smaller than other cases. But for the larger hole sizes, the increase was significantly high (e.g. 48% increase for 0.6" diameter).

In the case of plexiglass reinforcement the improvement was relatively small because of material property. However, it was higher than tension case because of the load direction which caused more interaction between plug and hole.

The results of steel inclusion also showed large amount of improvement as in aluminum case. This phenomenon is the different than in tension case. This can be attributed again to increased interaction between plug and hole during compression.

Failure Mechanism Analysis. Failure initiation and growth for unbonded tension tests was very similar to bonded case. The X-ray pictures of typical failure in unbonded tension specimen at 70 and 88% of failure load are shown in Fig. 27 and 28. As it can be seen from these figures, the failure has already started somewhere before 70% of failure load. And it progressed with further increase in load.

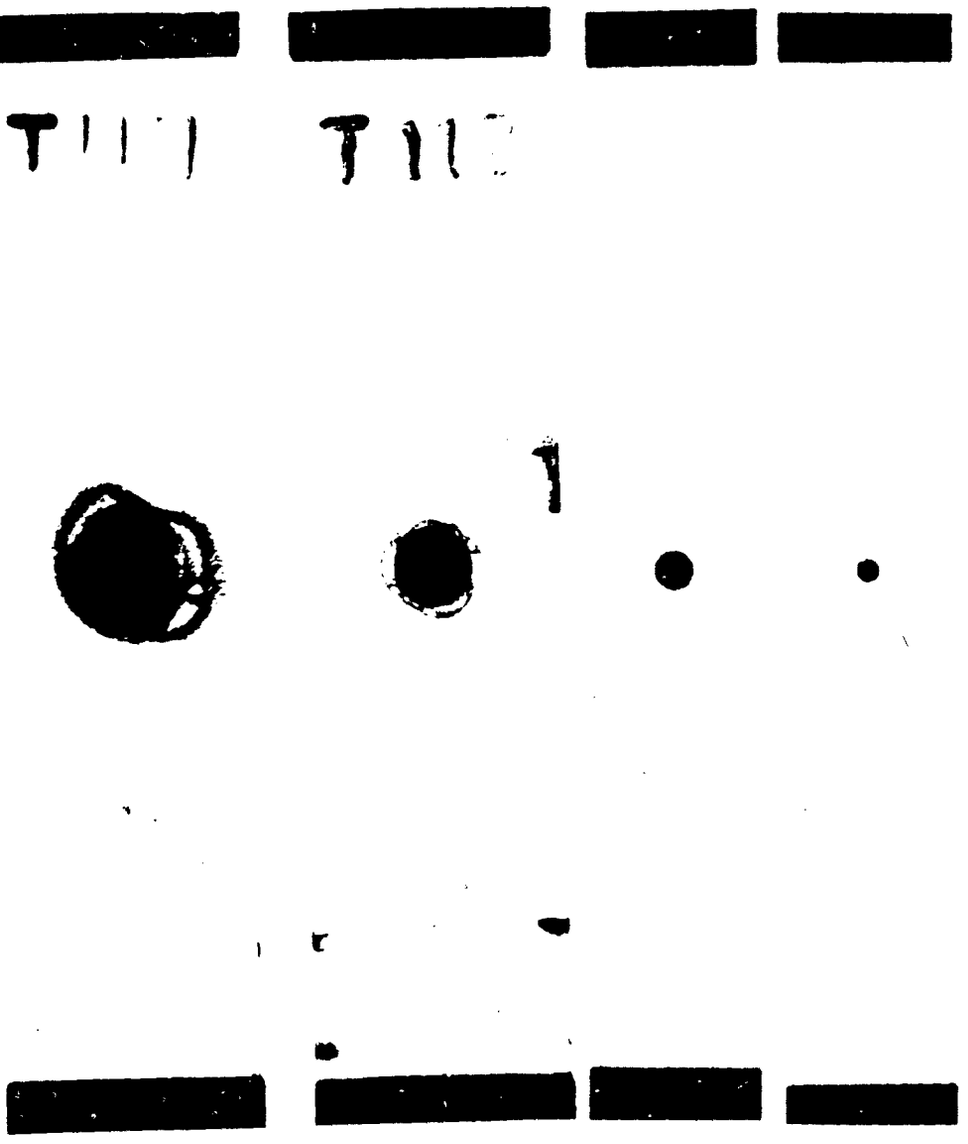

Fig. 27. X-Ray Results of Unbonded Aluminum Reinforcement under Tension Test (70% of Failure Load).

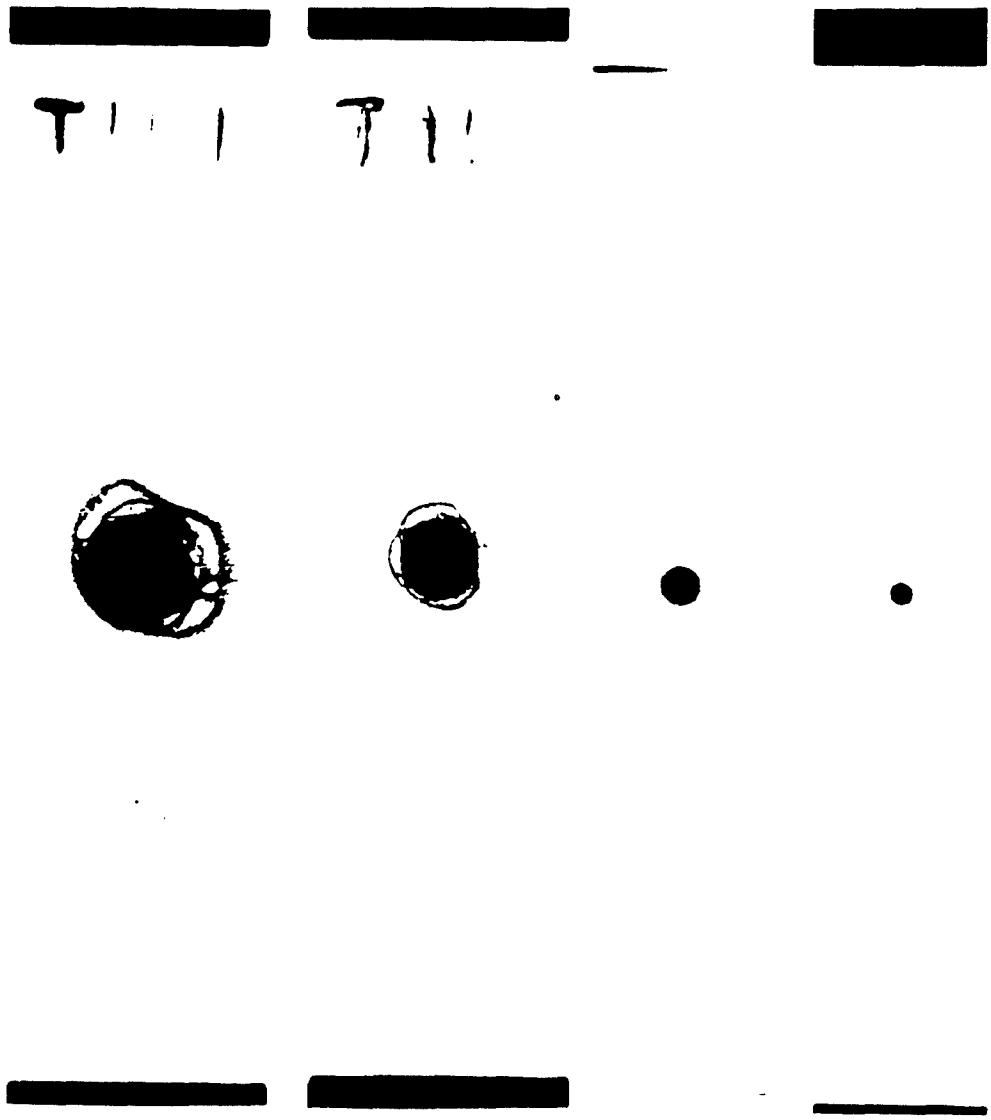

Fig. 28. X-Ray Results of Unbonded Aluminum Reinforcement under Tension Test (88% of Failure Load).

In compression test, the load transfer mechanism between plug and hole is much different than tension test case. As mentioned before, the load is mainly transferred through the top and bottom portion of the hole during compression loading. As shown in Figs. 29 through 32, crack initiated at 0 degree direction relative to the load axis, and grew, in general, in that direction, increasing load. In case of tension test, 90^0 matrix failed at about 50% of the ultimate load, but in compression case, no matrix or fiber failed until ultimate failure of laminate was occurring.

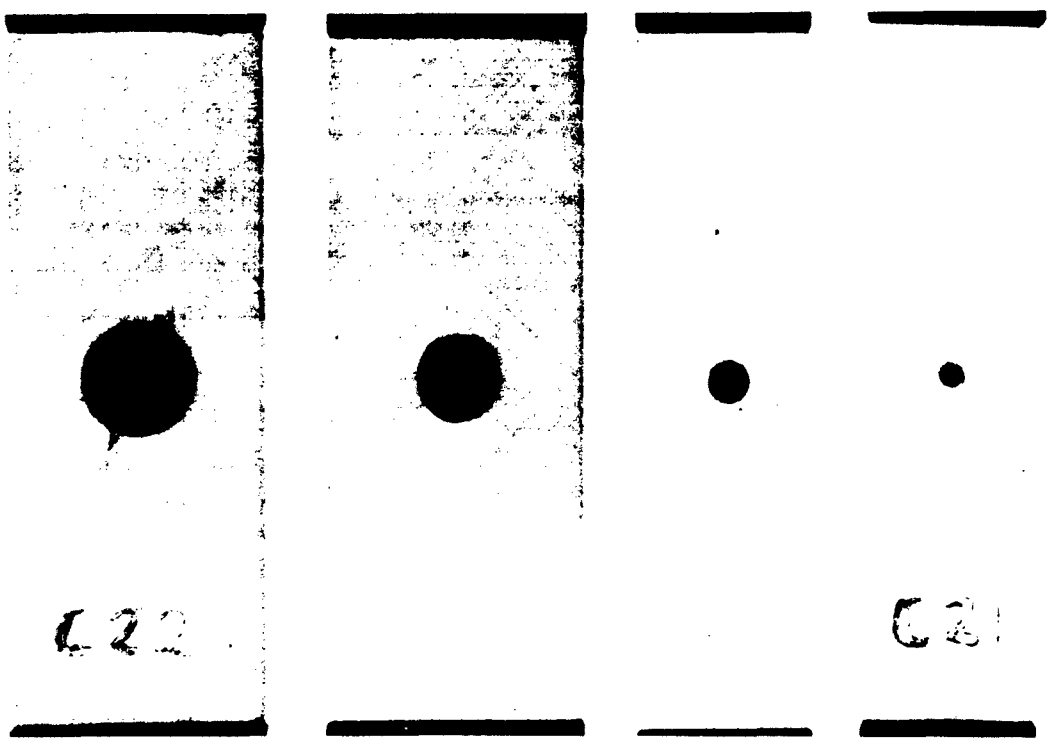

Fig. 29. X-Ray Result of Unbonded Aluminum Reinforcement under Compression Test (0% Load).

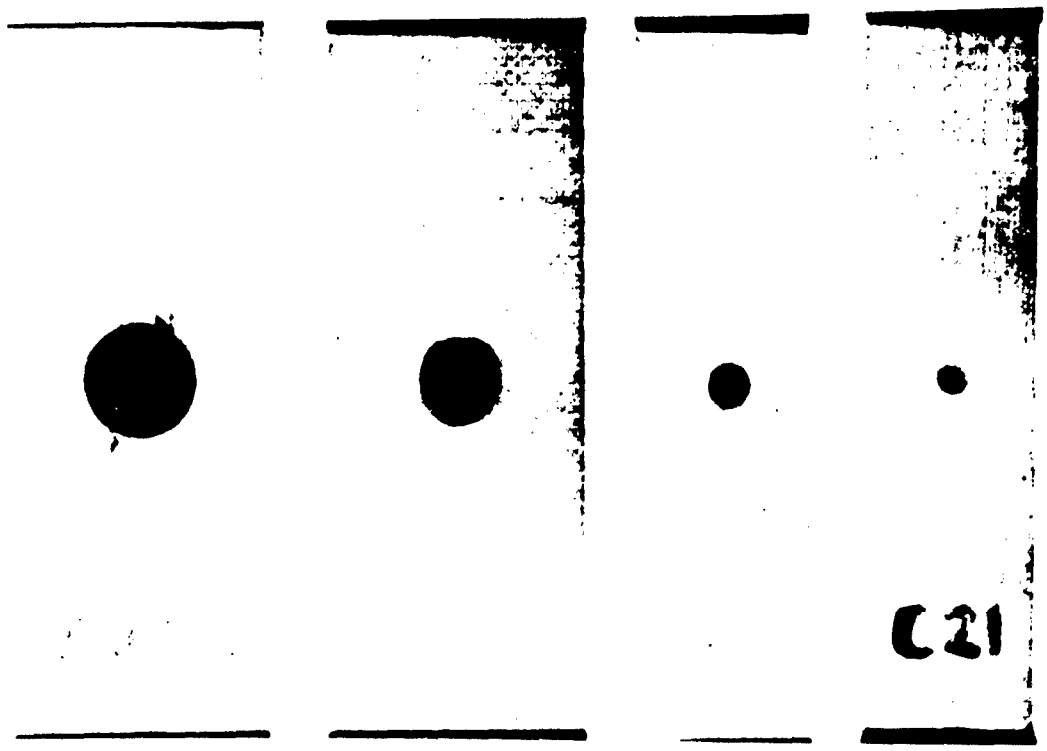

Fig. 30. X-Ray Result of Unbonded Aluminum Reinforcement under Compression Test (50% Load).

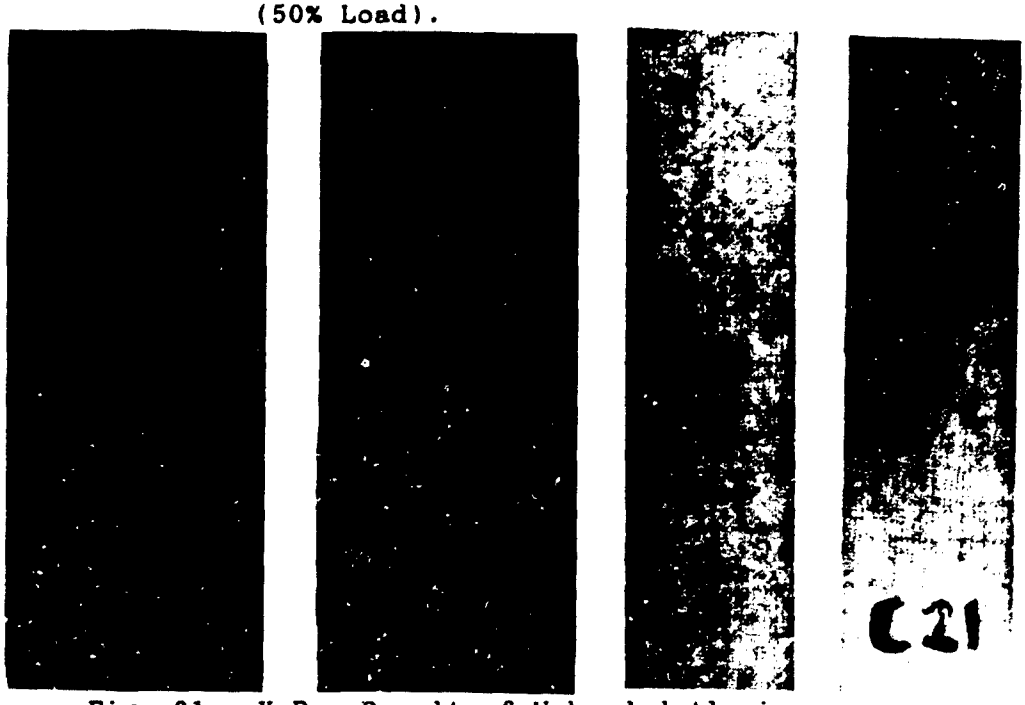

Fig. 31. X-Ray Result of Unbonded Aluminum Reinforcement under Compression Test (71% Load).

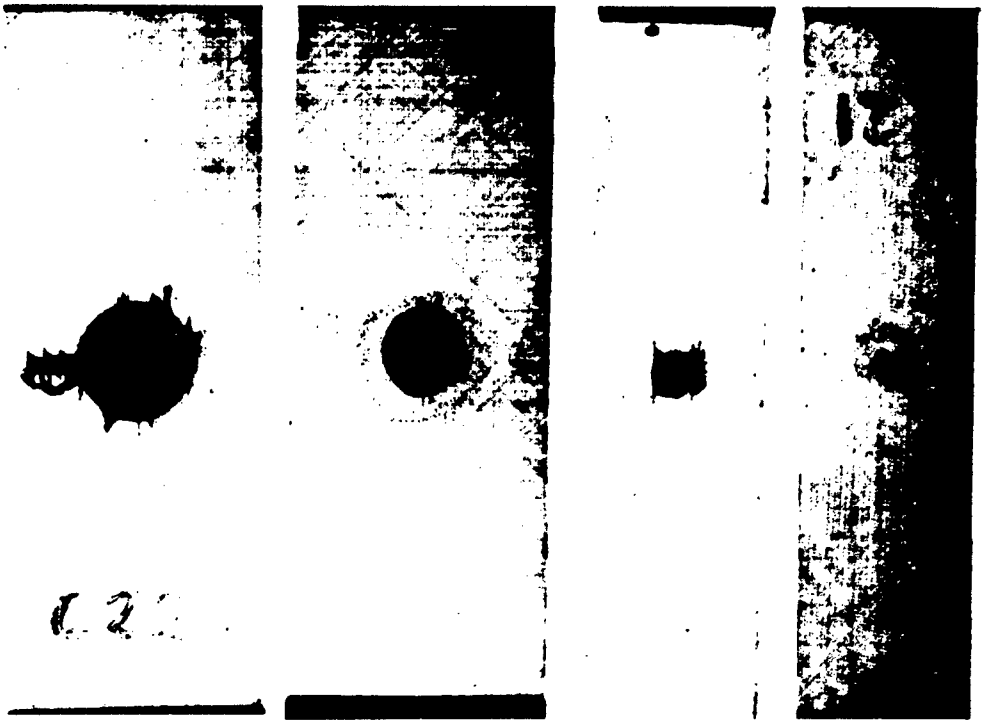

Fig. 32. X-Ray Result of Unbonded Aluminum Reinforcement under Compression Test (93% Load).

During compression test also, as in tension test case, the plexiglass reinforcement was broken as soon as the specimen failed. On the contrary, in case of steel reinforcement, the plug did not show any deformation at all. For the aluminum reinforcement, the plug deformed quite a bit depending on the loading condition. For tension test, deformation was very small and it was hard to find with naked eyes. In the case of compression, the deformation of plug was much greater than tension case, especially for small diameter. Figure 33 and 34 shows magnified picture of the typical deformed aluminum plug after tension and compression test.

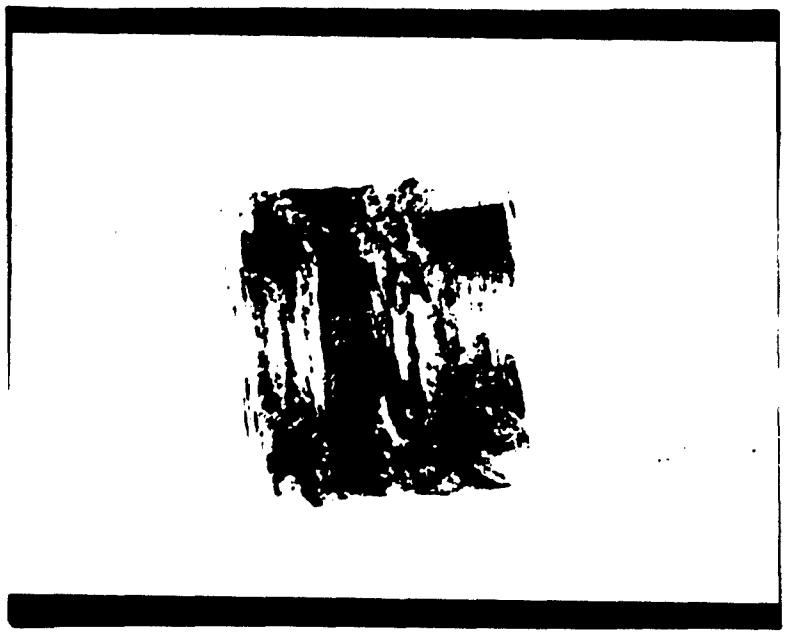

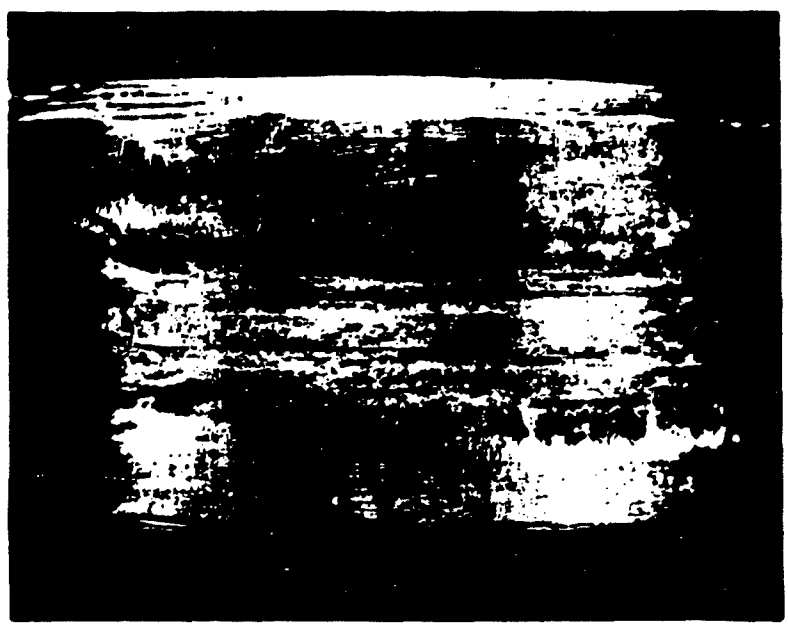

Fig. 33. Deformation of Reinforcement under Compression (Up: 0.2" Aluminum, Down: 0.6" Aluminum, X30.)

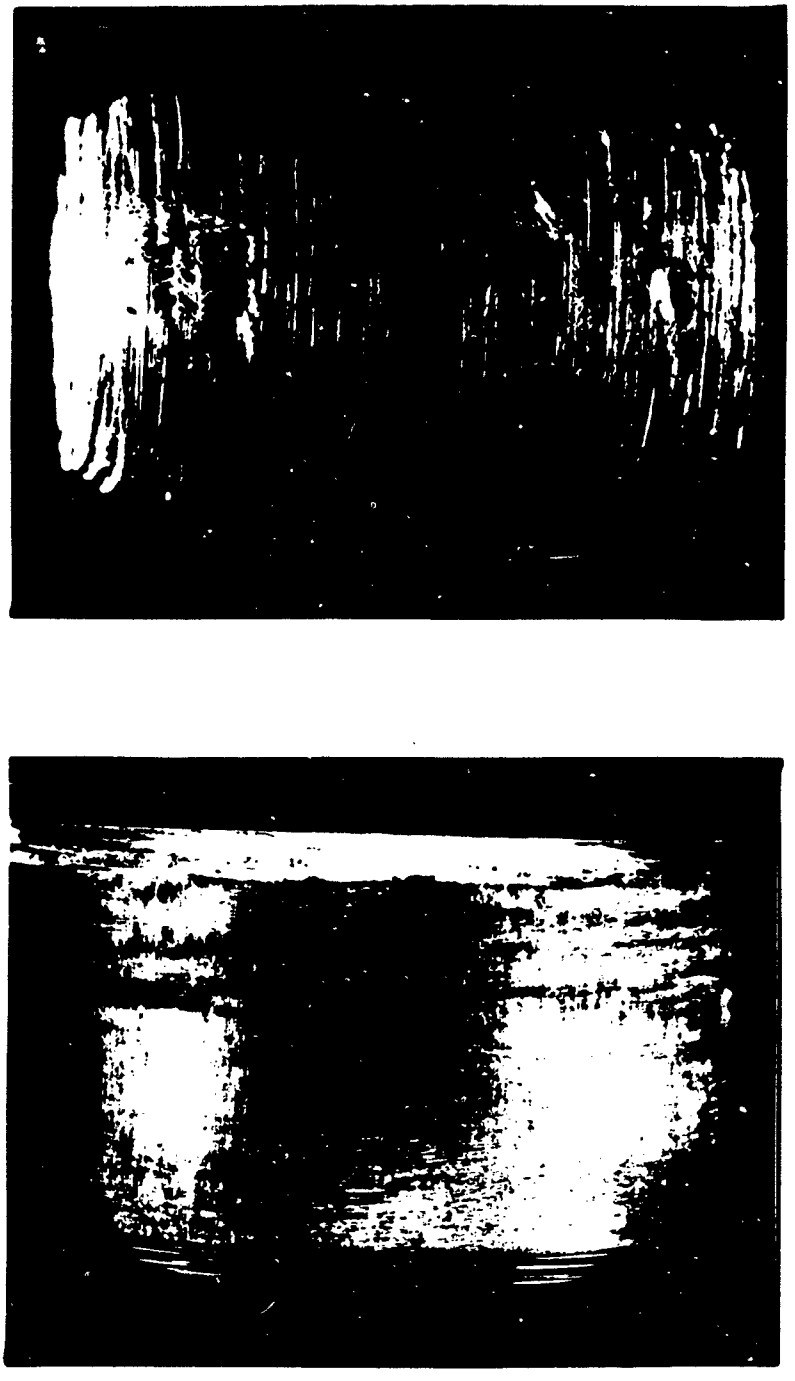

Fig. 34. Deformation of Reinforcement under Tension (Up: 0.2" Aluminum, Down: 0.6", X30).

Comparison With Strength Prediction Models

The test results of present study will be compared with the strength prediction models developed by Tan (21) which were discussed in detail in Chapter III. The comparison of notched strength prediction for open hole showed very good agreement with experimental data from his study, as shown in Fig. 5. However, experimental results of reinforced hole did not agree with these prediction models (as will be shown below). This can be attributed to the fact that theoretical models are based on perfect bonding. But if we adjust characteristic length of each prediction model, we probably can get certain agreement between theoretical prediction and experimental data. In this section, as a sample, experimental results of aluminum and steel are applied to Mininum Strength Model(MS) which is given below.

Minimum Strength Model (MS). In MS model the characteristic length, b_0, is measured radially from crack opening as shown in Fig. 1. In case of quasi-isotropic laminate with open hole, the characteristic lengths were as follows (21).

Criteria	Tension	Compression
FPF	0.03"	0.02"
FF	0.025"	0.025"

The results of aluminum reinforcement for tension and compression are plotted in Figs. 35 and 36 along with predicted values from this model based on perfect bonding

from FPF and FF criteria. Also these figures show the adjusted characteristic length, b_o which makes best fit with experimental data for each criterion along with its predicted values of strength reduction factor (SRF).

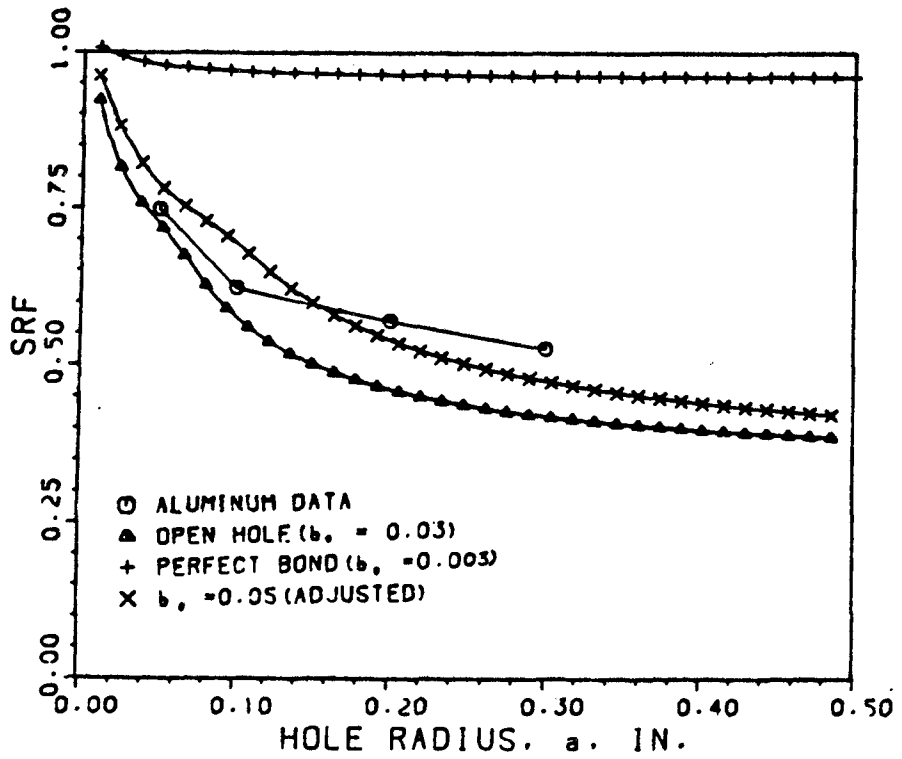

(a) First Ply Failure (FPF) Criterion.

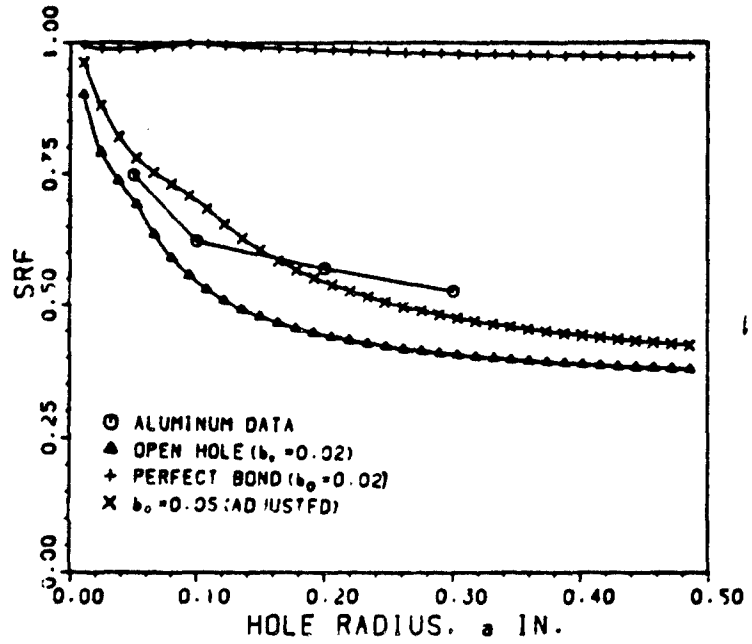

(b) Fiber Failure (FF) Criterion.

Fig. 35. Comparison of Tension Test Data of Unbonded Aluminum Reinforcement with MS Model.

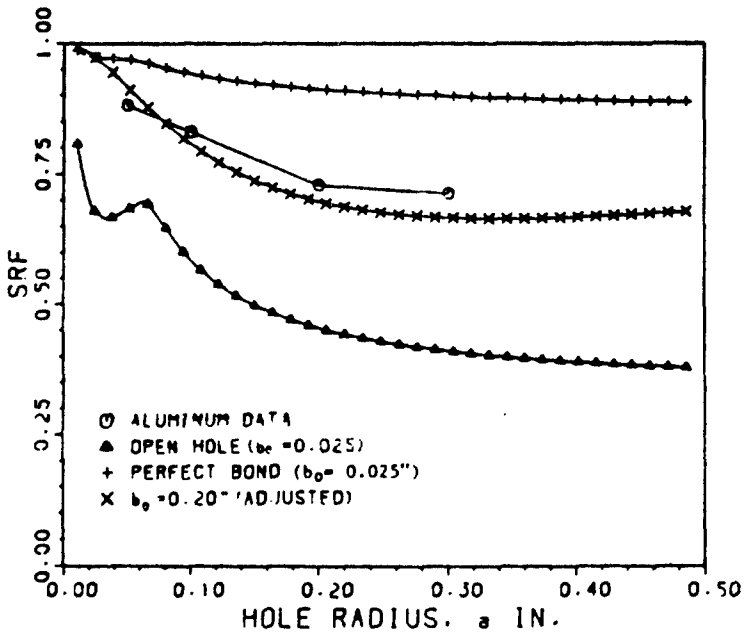

(a) First Ply Failure (FPF) Criterion.

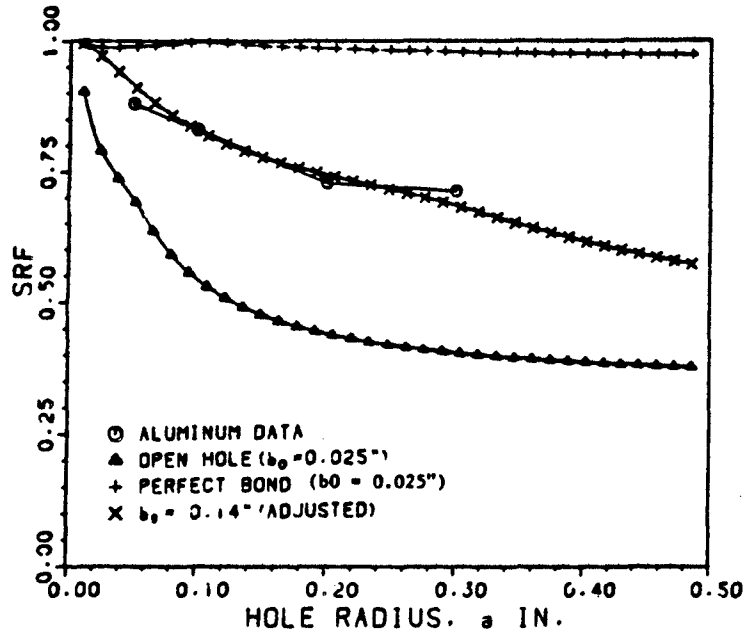

(b) Fiber Failure (FF) Criterion.

Fig. 36. Comparison of Compression Test Data of Unbonded Aluminum Reinforcement.

In tension, the improvement with reinforced hole was relatively small thus the adjusted characteristic length is also small. For both criteria (PFP and FF) with b_0 = 0.05" showed good agreement with test data. For compression test case, the improvement was much higher than tension, therefore, adjusted characteristic length is also much different than tension case. The FPF criterion (b_0 = 0.20") and FF criterion (b_c = 0.15") showed good agreement with experimental data.

Figs. 37 and 38 shows the similar comparison with results of steel inclusion from both tension and compression tests with predicted values from this model based on prefect

bonding between hole and reinforcement. Further, these are compared with predicted values with adjusted characteristic length, b_o.

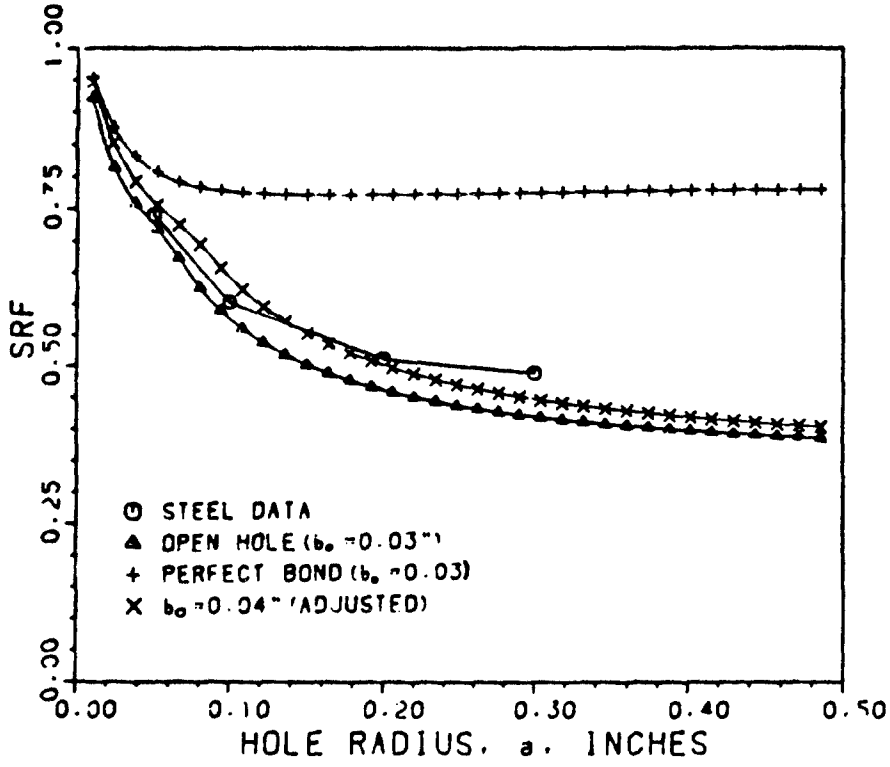

(a) First Ply Failure (FPF) Criterion.

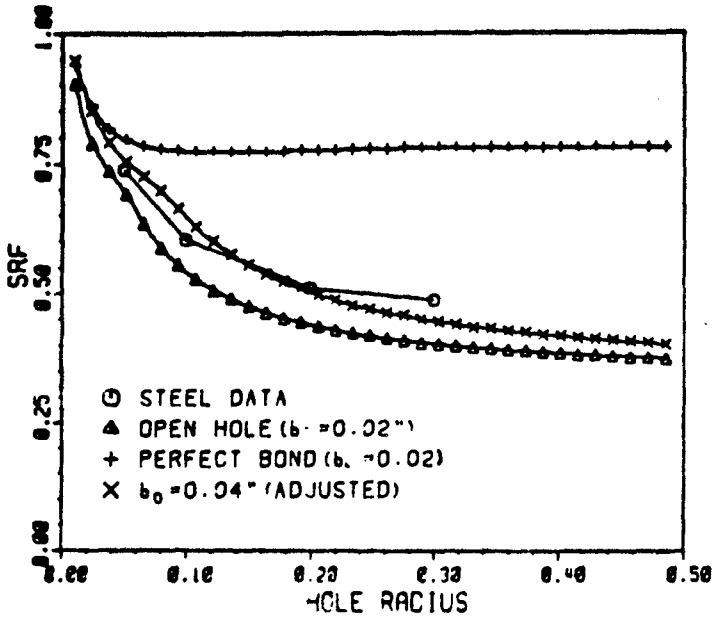

(b) Fiber Failure (FF) Criterion.

Fig. 37. Comparison of Tension Test Data of Unbonded Steel Inclusion with MS Model.

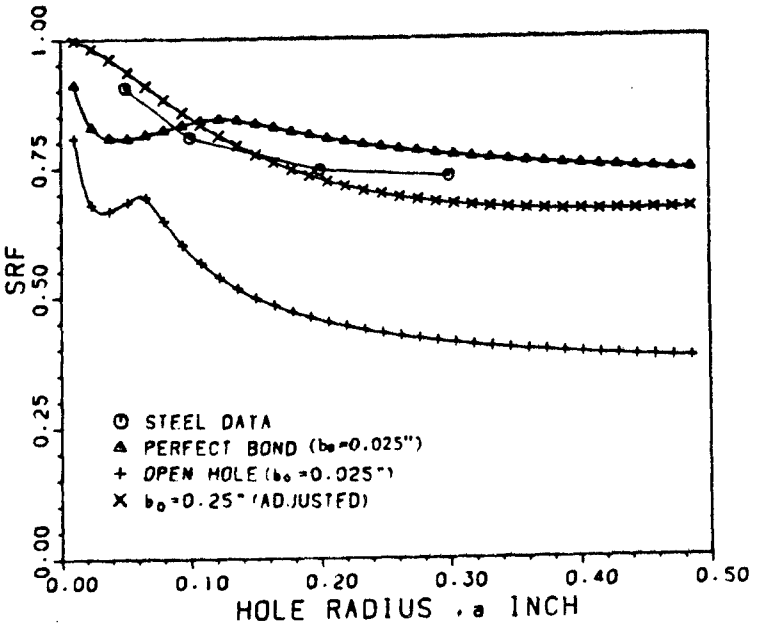

(a) First Ply Failure (FPF) Criterion.

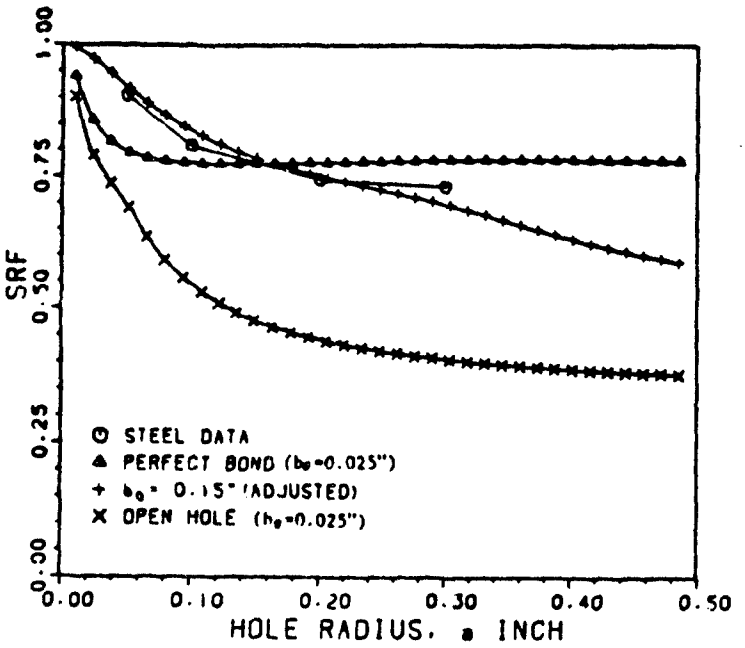

(b) Fiber Failure Criterion (FF).

Fig. 38. Comparison of Compression Test Data of Unbonded Steel Inclusion with MS Model.

In case of tension with steel inclusion, the results are almost same as aluminum reinforcement except for different b_0 = 0.04" (for both FPF, FF). For compression, test results also showed good agreement for both criteria (b_0 = 0.25" for FPF, b_0 = 0.15" for FF), however for the hole radius less than approximately 0.12", the tests results showed higher value than predicted value from model with perfect bonding.

VI. Conclusions

The following conclusions can be drawn from the present study:

1. In general, the composite laminate with a reinforced hole showed improvement of ultimate strength relative to the laminate with open hole.

2. The aluminum reinforcement showed the largest improvement out of all reinforcing materials and especially under compression loading. This improvement depended on the size of reinforcement. In general, the larger size of reinforcement showed more improvement.

3. With plexiglass reinforcement, the improvement of ultimate strength was very small because of the property of material.

4. The steel reinforcement showed almost same amount of increase in ultimate strength as aluminum in compression but showed less improvement in tension.

5. The composite laminate with bonded reinforcement showed practically no increase in ultimate strength because of adhesive failure. Thus, if a strong bondline between reinforcement and plug could be developed, the ultimate strength is expected to increase better than unbonded reinforcement.

6. The strain near the hole with reinforcement showed the linear response until failure.

7. In most cases the application of experimental data to the previously developed strength prediction model showed good agreement with analytical solution by adjusting the characteristic length from that of open hole.

Bibliography

1. Engineering Science Data Unit, Item 7005, Elastic Stress Concentration Factors of Single Reinforced and Unreinforced Holes in Infinite Plates of Isotropic Materials, 1970.

2. Timoshenko and Goodier, J. E. Theory of Elasticity. Engineering Society Monograph, 1951.

3. Lekhnitakii, S. G. Anisotropic Plates. Translated from the Second Russian Edition by S. W. Tsai and T. Cheorn, Gordon and Breach, Science Published Inc., New York, p. 157, 1968.

4. Cruse, T. A. "Tensile Strength of Notched Composites," Journal of Composite Materials, 7. (April 1973).

5. Pipes, R. B., Wetherhold, R. C. and Gillespie, J. W. "Notched Strength of Composite Materials," Journal of Composite Materials, 13. (April 1979).

6 Karlak, R. F. "Hole Effects in Related Series of Symmetrical Laminates," Material Science and Engineering, 41: 105, 1979.

7. Tan, S. C. "Notched Strength Prediction and Design of Laminated Composite Under In-Plane Loadings," Journal of Composite Materials, 21. (October 1987).

8. Mar, J. W. and Lagace, P. A. "Tensile Fracture of Gr/Ep Laminates with Holes," in Preceedings of Third International Conference on Composite Materials (ICCM-III), pp. 130-145, Paris, France 1980.

9 Kocher, L. H. and Cross, S. L. "Reinforced Cutouts in Graphite Composite Structures," Composite Materials (2nd Conference) ASTM STP 497, p. 382, 1972.

10. O'Neill, S. S. Asymmetric Reinforcement of a Quasi-Isotropic Gr/Ep Plates Containing a Circular Hole. MS thesis, Naval Post Graduate School, Monterey, CA, 1982.

11. Pickett, D. H. and Sullivan, P. D. Analysis of Symmetrical Reinforcement of Quasi-Isotropic Gr/Ep Plates With a Circular Cutout Under Uniaxial Tension Loading. MS thesis, NPGS, Monterey, CA. (December 1983).

12. Tan, S. C. and Tsai, S.W. Notched Strength. Composites Design, 3d Edition, 1987.

13. Waddoups, M. E., Eisenmann, J. R. and Kaminski, B.E. "Macroscopic Fracture Mechanics of Advanced Composite Materials," Journal of Composite Materials, 5:446. (1971).

14. Bowie, O. L. "Analysis of Infinite Plate Containing Radial Cracks Originating from the Boundary of an Internal Circular Hole," Journal of Mathematics and Physics, 35:60. (1956).

15. Whitney, J. M. and Nuismer, R.J. "Stress Fracture Criteria for Laminated Composites Containing Stress Concentrations," Journal of Composite Materials, 8. (July 1974).

16. Whitney, J. M. and Nuismer, R. J. "Uniaxial Failure of Composite Laminates Containing Stress Concentrations," ASTM STP 593, 1975.

17. Whitney, J. M. and Kim, R. Y. Effect of Stacking Sequence on the Notched Strength of Composite Laminates. AFML-TR-76-177 (November 1976).

18. Pipes, R.B., Gillipse, J. R. and Wethhold, R. C. "Superposition of the Notched Strength of Composite Laminates," Polymer Engineering and Science, 19. (December 1979).

19. Malik, B. U. Strength and Failure Analysis of Composite Laminates with Holes at Room and Elevated Temperature. MS thesis, AFIT/GAE/AA/84-12. School of Engineering, Air Force Institute of Technology (AU) Wright-Patterson AFB OH, December 1984.

20. Ramey, J. Comparison of Notched Strength Between Gr/PEEK (APC-1 and APC-2) and Gr/Epoxy Composite Material at Elevated Temperature. MS thesis, AFIT/GAE/AA/85D-12. School of Engineering, Air Force Institute of Technology (AU) Wright-Patterson AFB OH, December 1985.

21. Tan, S. C. "Effective Stress Fracture Models for Unnotched Multi-directional Laminates," Journal of Composite Materials, 21. (November 1987).

22. Gurney, C. "An Analysis of Stresses in a Flat Plate with a Reinforced Hole Under Edge Forces," Aeronautical Research Committee R. and M. No. 1834, London, 1938.

23. Reissner, H. and Murduchow, M. "Reinforced Circular Cutouts in Plane Sheets," NACA TN 1852, 1949.

24. Mansfield, E. H. "Neutral Holes in Plane Sheet-Reinforced Holes Which Are Elastically Equivalent to the Uncutsheet," Quarterly Journal of Mechanics and Applied Mathematics, IV:370. (1953).

25. Seika, M. and Ishii, M. "Photo Elastic Investigation of the Maximum Stress in a Plate with a Reinforced Circular Hole Under Uniaxial Tension," Trans. ASME 86 E (1964) Applied Mechanics Section, p. 701.

26. Ghosh, S. P., Dattaguru, B. and Rao, A. K. "Stresses Due to Variable Interference and Clearance Fit Pins in Large Sheets," Journal of Aerospace Society of India, 36, No. 1. (1983).

27. Heller, M. and Jones, R. "Analysis of Bonded Inserts for the Repair of Fastener Holes," Engineering Fracture Mechanics, 24:523. No. 4. (1986).

28. Waszczak, J. P. and Cruse,T. A. "Fracture Mode and Strength Predictions of Anisotropic Bolt Bearing Specimens," Journal of Composite Materials, 5:421. (July 1971).

29. Pradhan, B. and Kumar, Ray. "Stress Around Partial Contact Pin-Loaded Holes in FRP Composite Plates," Journal of Reinforced Plastics and Composites, 3. (January 1984).

30. Pradhan, B. and Santra, M. L. "Hole Reinforcement for Reducing SCF in Uniaxially Loaded FRP Composite Plate Containing Central Circular Holes," Fibre Science and Technology (England), 21:149-160. (1984).

31. Chang, F. K. "The Effect of Pin Load Distribution on the Strength of Pin Loaded Holes in Laminated Composites," Journal of Composite Materials, 20. (July 1986).

32. Chang, F. K., Scott, R.A. and Springer, G.S. Strength of Bolted Joints in Laminated Composites, Air Force Wright Aeronautical Laboratories, Technical Report, AFWAL-TR-4029 (1984).

33. Chang, F. K., Scott, R. A. and Springer, G. S. "Strength of Mechanically Fastened Composite Joints," Journal of Composite Materials, 16:470-494. (1982).

34. Hyer, M. W., Klang, E. C. and Cooper, D. E. "The Effects of Pin Elasticity, Clearance, and Friction on the Stresses in a Pin-Loaded Orthotropic Plate," Journal of Composite Materials, 21. (March 1987).

35. Awerbuch, J. and Madhukar, M. S. "Notched Strength of Composite Laminates; Prediction and Experiments - A Review," Journal of Reinforced Plastics and Composites, 4. (1985).

36. Aronsson, C. G. and Backlund, J. "Tensile Fracture of Laminates With Cracks," Journal of Composite Materials, 20:287-307. (1986).

37. Tan, S. C. "Laminated Composites Containing an Elliptical Opening, I. Approximate Stress Analysis and Fracture Modes," Journal of Composite Materials, 21. (November 1987).

VITA

Jong Hee Lee, was born 15 March 1959 in Village Nokjeon, Andong. He graduated from Kum-Oh Technical High School in 1977. After receiving a Bachelor of Science in Mechanical Engineering from Air Force Academy, Korea, he served as Weapon Systems Officer of F-4D fighter aircraft at various Korean Air Force bases. In June 1986, he entered the Air Force Institute of Technology in the Graduate Aeronautical Engineering Program.

Permanent Address: 130-14
Songnamsi Dandaedong 3277
Seoul, Korea.

SECURITY CLASSIFICATION OF THIS PAGE

REPORT DOCUMENTATION PAGE

Form Approved OMB No. 0704-0188

1a. REPORT SECURITY CLASSIFICATION: UNCLASSIFIED	1b. RESTRICTIVE MARKINGS
2a. SECURITY CLASSIFICATION AUTHORITY	3. DISTRIBUTION/AVAILABILITY OF REPORT: Approved for public release; distribution unlimited.
2b. DECLASSIFICATION/DOWNGRADING SCHEDULE	
4. PERFORMING ORGANIZATION REPORT NUMBER(S): AFIT/GAE/AA/87D-9	5. MONITORING ORGANIZATION REPORT NUMBER(S)
6a. NAME OF PERFORMING ORGANIZATION: School of Engineering; 6b. OFFICE SYMBOL (If applicable): AFIT/ENG	7a. NAME OF MONITORING ORGANIZATION
6c. ADDRESS (City, State, and ZIP Code)	7b. ADDRESS (City, State, and ZIP Code)
8a. NAME OF FUNDING/SPONSORING ORGANIZATION; 8b. OFFICE SYMBOL (If applicable)	9 PROCUREMENT INSTRUMENT IDENTIFICATION NUMBER
8c. ADDRESS (City, State, and ZIP Code)	10. SOURCE OF FUNDING NUMBERS: PROGRAM ELEMENT NO. / PROJECT NO. / TASK NO / WORK UNIT ACCESSION NO.

11. TITLE (Include Security Classification)

STRENGTH AND FAILURE ANALYSIS OF COMPOSITE LAMINATE CONTAINING A CIRCULAR HOLE WITH REINFORCEMENT

12. PERSONAL AUTHOR(S)

Jong Hee Lee, B.S., Capt, ROKAF

13a. TYPE OF REPORT	13b. TIME COVERED	14. DATE OF REPORT (Year, Month, Day)	15. PAGE COUNT
MS Thesis	FROM _____ TO _____	1987 December	105

16. SUPPLEMENTARY NOTATION

17. COSATI CODES			18. SUBJECT TERMS (Continue on reverse if necessary and identify by block number)
FIELD	GROUP	SUB-GROUP	Composite Materials, Bonding, Openings, Strength, Reinforcement
13	05		

19. ABSTRACT (Continue on reverse if necessary and identify by block number)

[illegible] AFR 190-1
31 Dec 87
[illegible] Development

Thesis Chairman: Shankar Mall, Dr

Professor of Aeronautical Engineering

20. DISTRIBUTION/AVAILABILITY OF ABSTRACT	21 ABSTRACT SECURITY CLASSIFICATION
☐ UNCLASSIFIED/UNLIMITED ☒ SAME AS RPT ☐ OTIC USERS	UNCLASSIFIED

22a. NAME OF RESPONSIBLE INDIVIDUAL	22b TELEPHONE (Include Area Code)	22c. OFFICE SYMBOL
Shankar Mall, Dr	(513) 237-7942	AFIT/ENY

DD Form 1473, JUN 86 *Previous editions are obsolete.*

SECURITY CLASSIFICATION OF THIS PAGE

UNCLASSIFIED

Tension and compression tests of quasi-isotropic, $[0/\pm45/90]_{2s}$ graphite/epoxy laminate containing circular hole with reinforcement was conducted using Instron static testing machine. Two types of reinforcement boundary conditions were investigated; adhesive bond reinforcement and snug-fit unbonded plug. For each case boundary conditions, four different sizes of hole diameter (0.1",0.2",0.4",0.6") and three types of reinforcing material(aluminum,plexiglass,steel) were employed for investigation.

The experiments were mainly focused on the evaluation of ultimate strength of reinforced panel relative to the case of open hole. In addition to this, failure mechanism analysis for both boundary conditions were studied. To help designers and users of composite, previously available theoretical fracture models and their comparison with the present experimental results are also discussed.